Journal of Medicinal Chemistry

Article

Cite This: J. Med. Chem. XXXX, XXX, XXX−XXX

pubs.acs.org/jmc

Synthesis and Biological Evaluation of Selenium-Containing 4-Anilinoquinazoline Derivatives as Novel Antimitotic Agents

Baijiao An, Bo Wang, Jinhui Hu, Shaoyu Xu, Ling Huang,* Xingshu Li,* and Albert S. C. Chan

School of Pharmaceutical Sciences, Sun Yat-sen University, Guangzhou 510006, China

Supporting Information

ABSTRACT: Twenty-eight novel selenium-containing 4-anilinoquinazoline derivatives were designed, synthesized, and evaluated as antiproliferative agents. Most of them had significant in vitro activities, particularly for compounds **23a**, **25a**, and **25d**, which also exhibited the most potent antitumor activities against cisplatin-resistant cell lines and the doxorubicin-resistant cell lines, good selectivity toward normal cells, and obvious inhibitory effect on migration of A549 cell lines. Further mechanistic studies revealed that **23a**, **25a**, and **25d** induce G2/M phase arrest and apoptosis in A549 cells, which was associated with a collapse of the mitochondrial membrane potential, alterations in the expression of some cell cycle-related and apoptosis-related proteins, and increasing the intracellular ROS level. Finally, compounds **23a**, **25a**, and **25d** also effectively inhibited the tumor growth in the A549 xenograft model without obvious hints of toxicity. Taken together, these in vitro and in vivo results suggest that **23a**, **25a**, and **25d** may be promising microtubule-stabilizing agents and can be used as a promising lead for the development of new antitumor agents.

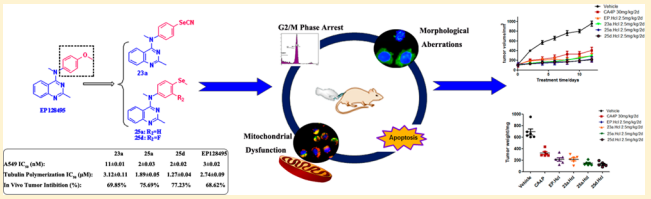

INTRODUCTION

The high incidence of cancer and the high cost of its treatment are important factors driving the search for new and effective chemotherapeutic substances with multitarget activity and no toxicity to normal cells. Among the variety of cancer drug targets, tubulin polymerization is an excellent choice as the microtubule system plays a critical role in essential cellular processes including the movement of organelles, intracellular transportation, and the formation and maintenance of cell shape.[1−4] In addition, several drugs (e.g., paclitaxel, docetaxel, and vinblastine) act on this target and have been used clinically,[5,6] and additional candidates are also in clinical trials. Among them, EP128495 (Figure 1), developed by Cai et.al., shows potent and broad-spectrum in vitro and in vivo cytotoxic activities and has reached a phase II clinical trial for the treatment of recurrent glioblastoma.[7,8]

Selenium (Se) is an essential trace mineral nutrient with multiple roles in human health.[9] It is known that 25 selenoproteins in the human body exert specific biological functions; for example, glutathione peroxidase, one of the selenoproteins, efficiently metabolizes cellular peroxides and functions as an antioxidant defense mechanism that protects against reactive oxygen and nitrogen species.[10] Selenium is also known to provide protection from free-radical-induced cell damage.[11] Numerous studies reported that the levels of selenium in humans are correlated with the incidence of many diseases. Selenium compounds have been used as promising chemopreventive agents for some diseases in the past few decades, including Keshan disease and Kashin−Beck disease.[12,13]

In recent years, the potential therapeutic effects of selenium for cancer treatment have attracted great interest. Some selenium compounds, including selenocyclodextrin, phenylbutyl isoselenocyanate, selenomethionine, sodium selenite, diaryl selenide, 3,4-diaryl-1,2,5-selenadiazol analogues, and selenoaspirin analogues, have been shown to inhibit cancer cell growth in vitro or in various xenograft rodent models for different cancers types.[14−21] Additionally, selenium has been reported to have a protective effect against some types of cancer and might also enhance male fertility in patients undergoing chemotherapy.[22] Recently, reports indicated that supplemental selenium may decrease ovarian cancer risk in African-American women, and selenium reduced doxorubicin gonadotoxicity in male rats.[23]

Inspired by the synergistic effects of organoselenium compounds in combination with chemotherapeutic drugs,[24−26] herein we report the modification of EP128495 by introducing selenocyanato or methylseleno at various positions of the anilino moiety of 4-anilinoquinazoline to obtain diverse derivatives. These derivatives were evaluated for antitumor activities in vitro and in vivo, and their underlying cytotoxic mechanisms were also elucidated

RESULTS AND DISCUSSION

Chemistry. The synthesis of new selenium-containing 4-anilinoquinazoline derivatives **7a−f** is shown in Scheme 1. First, 2-hydroxy-5-nitrobenzoic acid reacted with dimethyl sulfate and then was hydrogenated in the presence of Pd/C to give

Received: January 24, 2018

DOI: 10.1021/acs.jmedchem.8b00128
J. Med. Chem. XXXX, XXX, XXX−XXX

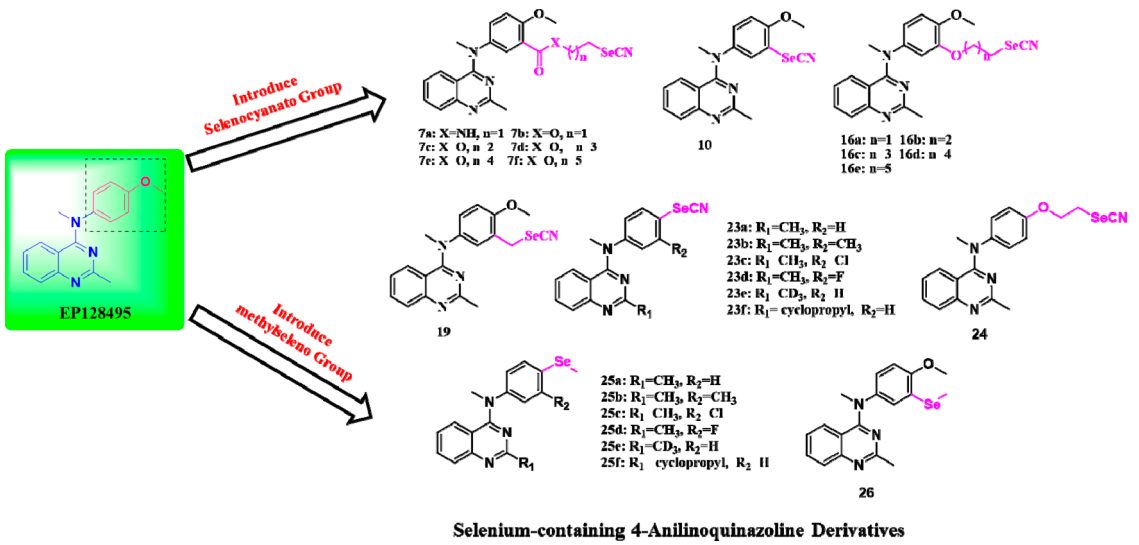

Figure 1. Design strategy of selenium-containing 4-anilinoquinazoline derivatives.

Scheme 1[a]

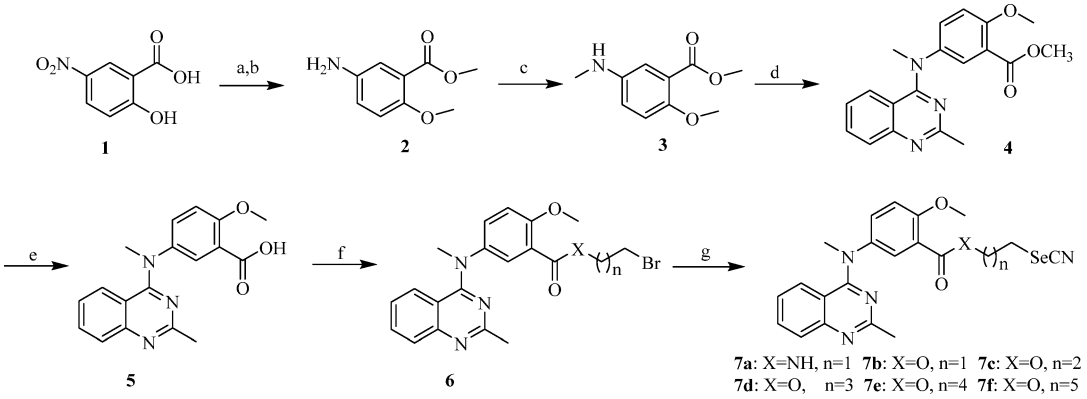

[a]Reagents and conditions: (a) K_2CO_3, dimethyl sulfate, acetone, 60 °C. (b) Pd/C, H_2, MeOH. (c) HAc, $(CH_2O)_n$, $NaBH_3CN$, rt. (d) 4-Chloro-2-methylquinazoline, HCl, IPA, rt. (e) NaOH, H_2O, MeOH, rt. (f) (1) $Br(CH_2)_nBr$, K_2CO_3, CH_3CN, reflux. (2) $SOCl_2$, $NH_2CH_2CH_2Br$, DCM. (g) KSeCN, CH_3CN, reflux.

Scheme 2[a]

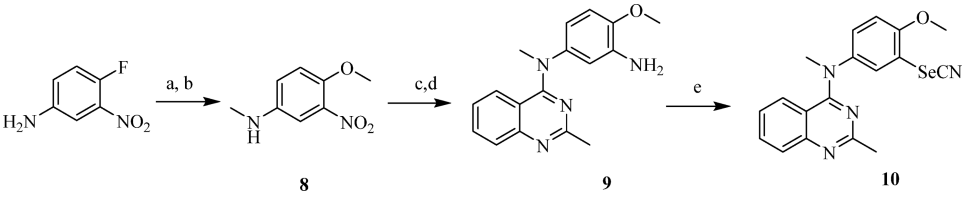

[a]Reagents and conditions: (a) Na, MeOH, reflux. (b) $(CH_2O)_n$, Na, $NaBH_4$, MeOH, 60 °C. (c) 4-Chloro-2-methylquinazoline, HCl, IPA. (d) Pd/C, H_2, MeOH. (e) HCl, $NaNO_2$, KSeCN.

intermediate **2**. The reactions of **2** with paraformaldehyde and sodium cyanoborohydride provided the secondary amine intermediate **3**. The reaction of **3** with 4-chloro-2-methylquinazoline and the following hydrolyzation produced the acid intermediate **5**. Finally, the esterification of intermediate **5** with the appropriate dibromoalkanes afforded compound **6** which was reacted with KSeCN to give the target products **7a**–**f**.

The synthesis of the target compounds **10**, **18**, and **21**, which contain 4-methoxy-3-selenocyanato at the anilino moiety or its analogues, is summarized in Schemes 2, 3, and 4. The reaction of 4-fluoro-3-nitroaniline with sodium methoxide in reflux gave 4-methoxy-3-nitroaniline, and the following alkylation afforded the key intermediate **8**. Compound **8** was reacted with 4-chloro-2-methylquinazoline and then hydrogenated in the presence of Pd/C to provide the intermediate **9**. Finally, the diazotization of **9** and the subsequently reaction with potassium selenocyanate afforded the target product **10** (Scheme 2).

The selenocyanato-containing compounds **16a**–**e** were synthesized as shown in Scheme 3. The hydrogenation of MOM-protected 2-methoxy-5-nitrophenol in the presence of Pd/C provided compound **12**, and subsequent alkylation gave the key intermediate **13**. By the reaction of **13** with 4-chloro-2-

DOI: 10.1021/acs.jmedchem.8b00128
J. Med. Chem. XXXX, XXX, XXX−XXX

Scheme 3[a]

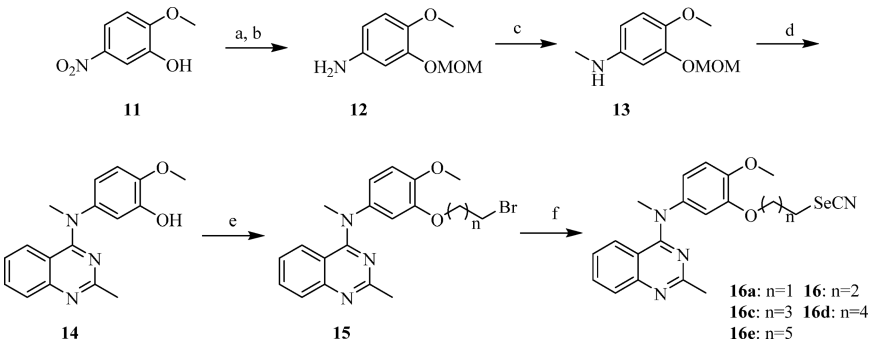

[a]Reagents and conditions: (a) MOMCl, DIPEA, DCM, 0 °C. (b) Pd/C, H_2, MeOH. (c) $(CH_2O)_n$, Na, $NaBH_4$, MeOH, 60 °C. (d) 4-Chloro-2-methylquinazoline, HCl, IPA. (e) K_2CO_3, $BrCH_2CH_2Br$, CH_3CN, reflux. (f) KSeCN, CH_3CN, reflux.

Scheme 4[a]

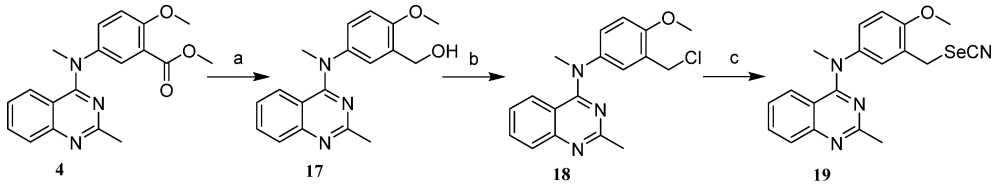

[a]Reagents and conditions: (a) $LiAlH_4$, THF, rt. (b) $SOCl_2$, reflux. (c) KSeCN, CH_3CN, reflux.

methylquinazoline, compound **14** was obtained. Finally, the reaction of **14** with the appropriate dibromoalkane and then with potassium selenocyanate afforded the target products.

Compound **19** was synthesized by the route shown in Scheme 4. The ester group of intermediate **4** was reduced with aluminum lithium hydride and then reacted with thionyl chloride to give compound **17**, which was converted to **18** by the same method above.

To investigate the role of selenium on the proliferative activity of human cancer cells, compound **20** was also prepared by the reaction of intermediate **15** with ammonium hydroxide (Scheme 5).

Scheme 5[a]

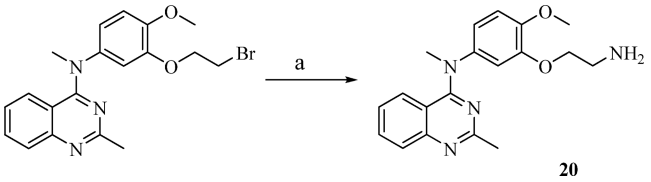

[a]Reagents and conditions: (a) NH_4OH, rt.

Compounds **23a–f**, for which selenocyanato is at the 4-position of the anilino moiety, were synthesized as Scheme 6. The alkylation of meta-substituted anilines by paraformaldehyde and sodium borohydride created compound **21**, which reacted with selenium dioxide and malononitrile to give **22**. Finally, compound **22** reacted with 4-chloroquinazoline to provide target compounds **23a–f**.

Compounds **25a–f**, in which the methylseleno is at the 4-position of the anilino moiety, were prepared by the reaction of **23** with sodium borohydride and methyl iodide (Scheme 7).

In Vitro Human Cancer Cell Line Growth Inhibition and the SARs. Recently, Sharma group reported the design and evaluation of Se-aspirin analogues as an effective agent in

Scheme 6[a]

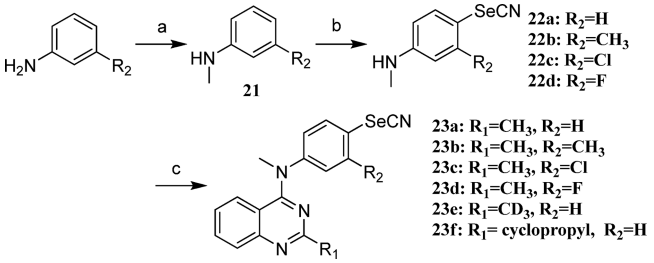

[a]Reagents and conditions: (a) $(CH_2O)_n$, Na, $NaBH_4$, MeOH, 60 °C. (b) Malononitrile, SeO_2, DMSO, rt. (c) 4-Chloro-2-methylquinazoline or its anlogues, HCl, IPA, rt.

Scheme 7[a]

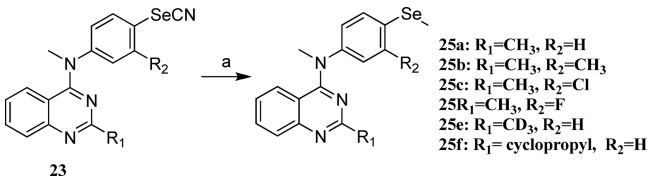

[a]Reagents and conditions: (a) MeI, $NaBH_4$, rt.

reducing the viability of different cancer cell lines, and among them, selenocyanato containing compounds exhibited the most antiproliferative activity.[21] Inspired by their work, we synthesized compounds **7a–f** and evaluated their antiproliferative activities against A549 (non-small-cell lung carcinoma), MDAMB-231 (human breast carcinoma), HepG2 (liver hepatocellular), HELA (human epithelial cervical cancer cell line), HCT116, LOVO, and RKO (human colorectal carcinoma) cell lines using the MTT (3-(4,5- dimethylthiazol-2-yl)-2,5-diphenyltetrazolium bromide) assay. As shown in Table 1, most of the compounds of this series exhibited good

DOI: 10.1021/acs.jmedchem.8b00128
J. Med. Chem. XXXX, XXX, XXX–XXX

Table 1. Antiproliferative Activity of Target Compounds against Six Human Cancer Cell Lines[a]

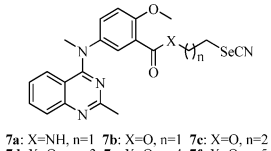

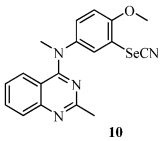

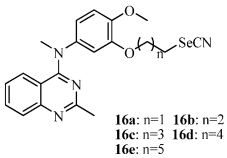

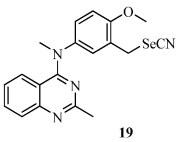

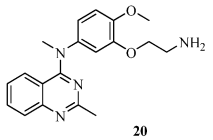

	IC_{50} (μM)[b]					
compd	A549	HCT116	HEPG2	MDAMB-231	LOVO	RKO
7a	0.187 ± 0.009	0.313 ± 0.013	0.179 ± 0.005	1.25 ± 0.025	0.561 ± 0.015	1.17 ± 0.036
7b	0.353 ± 0.013	0.951 ± 0.051	0.890 ± 0.012	1.48 ± 0.016	2.96 ± 0.087	2.39 ± 0.045
7c	0.250 ± 0.044	0.720 ± 0.015	0.34 ± 0.004	1.18 ± 0.013	0.854 ± 0.006	1.14 ± 0.034
7d	0.155 ± 0.009	0.662 ± 0.040	0.975 ± 0.008	0.554 ± 0.023	1.08 ± 0.060	1.02 ± 0.112
7e	0.592 ± 0.007	0.551 ± 0.005	0.667 ± 0.017	0.851 ± 0.018	0.714 ± 0.005	0.356 ± 0.011
7f	0.488 ± 0.018	1.99 ± 0.017	2.65 ± 0.097	2.21 ± 0.074	1.05 ± 0.092	1.99 ± 0.036
10	0.049 ± 0.014	0.034 ± 0.008	0.059 ± 0.005	0.052 ± 0.018	0.073 ± 0.006	0.047 ± 0.004
16a	0.013 ± 0.001	0.018 ± 0.004	0.014 ± 0.001	0.013 ± 0.005	0.019 ± 0.003	0.027 ± 0.067
16b	0.382 ± 0.004	0.852 ± 0.021	1.04 ± 0.012	0.815 ± 0.007	0.921 ± 0.015	0.799 ± 0.035
16c	1.20 ± 0.053	0.512 ± 0.009	6.46 ± 0.113	1.35 ± 0.024	0.882 ± 0.067	1.360 ± 0.059
16d	2.44 ± 0.033	0.256 ± 0.007	5.21 ± 0.024	4.41 ± 0.035	5.21 ± 0.006	3.56 ± 0.035
16e	5.52 ± 0.042	6.18 ± 0.023	4.89 ± 0.092	3.55 ± 0.016	8.58 ± 0.153	1.54 ± 0.062
19	0.098 ± 0.003	0.113 ± 0.011	1.11 ± 0.065	0.153 ± 0.011	0.277 ± 0.005	0.316 ± 0.031
20	0.122 ± 0.031	0.198 ± 0.004	0.343 ± 0.013	0.682 ± 0.003	0.421 ± 0.006	0.343 ± 0.005
EP128495	0.003 ± 0.002	0.004 ± 0.001	0.005 ± 0.002	0.008 ± 0.001	0.008 ± 0.0001	0.003 ± 0.0002

[a]Cell lines were treated with compounds for 48 h. Cell viability was measured by MTT assay as described in the Experimental Section. [b]IC_{50} values are indicated as the mean ± SD (standard error) of at least three independent experiments.

Table 2. Antiproliferative Activity of Target Compounds against Six Human Cancer Cell Lines[a]

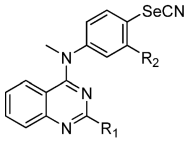

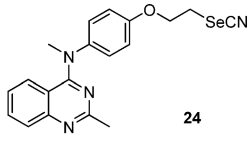

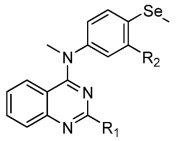

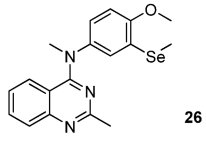

	IC_{50} (μM)[b]					
compd	A549	HCT116	HEPG2	MDAMB-231	LOVO	RKO
23a	0.011 ± 0.001	0.015 ± 0.001	0.009 ± 0.001	0.020 ± 0.0001	0.032 ± 0.003	0.009 ± 0.006
23b	0.008 ± 0.005	0.013 ± 0.004	0.009 ± 0.001	0.016 ± 0.003	0.019 ± 0.003	0.017 ± 0.002
23c	0.007 ± 0.002	0.012 ± 0.001	0.012 ± 0.001	0.009 ± 0.001	0.012 ± 0.003	0.011 ± 0.001
23d	0.004 ± 0.001	0.020 ± 0.002	0.037 ± 0.005	0.006 ± 0.0002	0.013 ± 0.003	0.008 ± 0.004
23e	0.007 ± 0.001	0.010 ± 0.004	0.021 ± 0.002	0.011 ± 0.001	0.014 ± 0.003	0.011 ± 0.004
23f	0.012 ± 0.007	0.062 ± 0.007	0.041 ± 0.002	0.029 ± 0.001	0.011 ± 0.003	0.051 ± 0.007
24	0.893 ± 0.031	2.29 ± 0.015	1.68 ± 0.098	0.317 ± 0.004	0.547 ± 0.006	0.652 ± 0.014
25a	0.002 ± 0.003	0.003 ± 0.002	0.004 ± 0.001	0.004 ± 0.001	0.009 ± 0.001	0.004 ± 0.001
25b	0.002 ± 0.001	0.003 ± 0.001	0.006 ± 0.001	0.007 ± 0.001	0.009 ± 0.001	0.008 ± 0.001
25c	0.002 ± 0.0004	0.005 ± 0.001	0.004 ± 0.001	0.007 ± 0.002	0.003 ± 0.001	0.004 ± 0.001
25d	0.002 ± 0.0001	0.006 ± 0.0001	0.004 ± 0.0002	0.005 ± 0.001	0.009 ± 0.0001	0.007 ± 0.0001
25e	0.003 ± 0.0001	0.003 ± 0.001	0.005 ± 0.0002	0.009 ± 0.001	0.005 ± 0.007	0.008 ± 0.001
25f	0.013 ± 0.001	0.015 ± 0.006	0.032 ± 0.006	0.018 ± 0.001	0.011 ± 0.003	0.021 ± 0.004
26	0.011 ± 0.001	0.028 ± 0.004	0.017 ± 0.002	0.010 ± 0.001	0.003 ± 0.005	0.011 ± 0.001
EP128495	0.003 ± 0.002	0.004 ± 0.001	0.005 ± 0.002	0.008 ± 0.001	0.008 ± 0.0001	0.003 ± 0.0002

[a]Cell lines were treated with compounds for 48 h. Cell viability was measured by MTT assay as described in the Experimental Section. [b]IC_{50} values are indicated as the mean ± SD (standard error) of at least three independent experiments.

antiproliferative activity with IC_{50} values at submicromolar level. However, reference compound EP128495 exhibits a more excellent antiproliferative activity, which urged us to search for potential compounds with better activities. We then evaluated

DOI: 10.1021/acs.jmedchem.8b00128
J. Med. Chem. XXXX, XXX, XXX−XXX

Table 3. Antiproliferative Activity of Optimal Compounds against Other Human Cancer Cell Lines[a]

	IC_{50} (μM)			
compd	23a	25a	25d	EP128495
MCF7	0.019 ± 0.006	0.010 ± 0.003	0.009 ± 0.004	0.011 ± 0.002
HELA	0.009 ± 0.002	0.003 ± 0.001	0.005 ± 0.001	0.005 ± 0.003
MGC803	0.012 ± 0.001	0.007 ± 0.002	0.007 ± 0.002	0.008 ± 0.001

[a]Data are presented as the mean ± SE from the dose−response curves of at least three independent experiments.

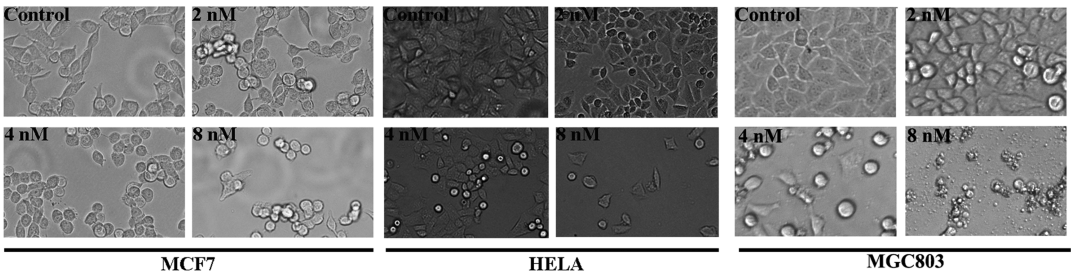

Figure 2. The human cancer cell lines were treated with **25a** at the indicated concentration or DMSO (0.01%) for 48 h, and the detection of the fixed cells morphology was performed with microscope. All images were collected with a 20× objective.

the antiproliferative activity of compounds **10**, **16**, and **19**, for which the selenocyanato is linked at the 3-position of the anilino moiety either directly or by a linker. The results in Table 1 showed that the position of the selenocyanato was important for the antiproliferative activity. Compound **10**, which has the selenocyanato linked directly at the 3-position of anilino moiety, exhibited very good activity with IC_{50} values that ranged from 34 to 73 nM against the six human cancer cell lines. The activity increased obviously when the selenocyanato was linked by a two-carbon ether chain (**16a**, IC_{50} values ranged from 13 to 27 nM) but decreased with an increase in the chain length (**16b**, n = 3, IC_{50} values ranged from 0.382 to 1.038 μM; **16e**, n = 5, IC_{50} values ranged from 1.541 to 8.583 μM), which revealed that the length of the linkage has a great effect on the inhibition of cancer cell proliferation. Compound **19**, in which the selenocyanato is linked at the 3-position of the anilino moiety via a methylene, had IC_{50} values that ranged from 0.098 to 1.105 μM, which is lower than that of compounds **10** and **16a**, suggesting that the ether chain is necessary in this series. Finally, by comparison of the IC_{50} values of **20** and **16a**, a difference of nearly 5 times the antiproliferative activity indicated that selenocyanato is indeed beneficial for the activity.

The antiproliferative activities of compounds **23a−f**, with selenocyanato at the 4-position of the anilino moiety with different substitutes at the 3-position, are listed in Table 2. All the members of this series of analogues exhibited excellent activities with IC_{50} values that ranged from 4 to 62 nM. There was not much activity difference against the six cancer cell lines, regardless of whether the substitutions at 3-position were hydrogen, methyl group, or a halogen. Similarly, the introduction of a CD_3 group at the R_1 position instead of a methyl group also gave nearly the same activities. As the presence of a cyclopropyl group is very crucial in many drugs, we introduced this group at the R_1 position to obtain compound **23f**. Compared with **23a**, we found the antiproliferative activities of **23f** were slightly decreased for some cancer cell lines. Compound **24**, in which the selenocyanato was linked via an ethyoxyl chain at the 4-position of the anilino moiety, had relatively poor antiproliferative activities which indicated that selenocyanato linked directly at the 4-position of the anilino moiety is necessary.

Considering the bioelectronic isostatic effect of selenium and oxygen, we introduced methylseleno at the 4-position of the anilino moiety to give compounds **25a−f**. The antiproliferative activity results summarized in Table 2 showed that most of the 4-methylseleno derivatives exhibited very good potencies compared to that of series of **7**, **16**, and **23**. Compounds **25a−d**, for which R_1 was a methyl group and the R_2 position contained H, CH_3, Cl, or F, exhibited very good antiproliferative activities that were not weaker than that of the reference compound EP128495. In contrast to the excellent activity of **25a−d**, compound **25f** provided relatively weaker potencies with IC_{50} values that ranged from 11 to 32 nM against the six human cancer cell lines, which indicated that the cyclopropyl group is not beneficial for antiproliferation activities at this position. Compound **26**, with the methoxyl group at the 4-position and methylseleno at the 3-position of the anilino moiety, gave slightly weaker antiproliferative activity compared to **25a−d** and showed that large groups at the 3-position might be not beneficial for potency.

23a, 25a, and 25d Inhibit Another Three Human Cancer Cell Lines and Alter Cell Morphology. As compounds **23a**, **25a**, and **25d** exhibited excellent antiproliferative activity in the initial cytotoxicity screening, we further evaluated their activities against another three different cancer cell lines [MCF7 (human breast carcinoma), HELA (human cervical carcinoma), MGC803 (human gastric adenocarcinoma)]. The results shown in Table 3 indicated that **23a**, **25a**, and **25d** also exhibited excellent antiproliferative activity with IC_{50} values in the low nanomolar range (IC_{50} = 3−19 nM). Additionally, the confocal image assays revealed that the compounds can highly alter cell morphology (Figure 2). All these data suggested that **23a**, **25a**, and **25d** were worthy of further study.

Antiproliferative Activity of 23a, 25a, and 25d against Drug-Resistant Cancer Cell Lines. Previous studies have shown that overexpression of P-glycoprotein (Pgp) in cancer cells can export anticancer drugs out and often cause clinical chemotherapy failure for anticancer drugs. To evaluate the anti-MDR potential of selenium-containing compounds **23a**, **25a**,

DOI: 10.1021/acs.jmedchem.8b00128
J. Med. Chem. XXXX, XXX, XXX−XXX

Table 4. Antiproliferative Activities of Optimal Compounds on the Cisplatin-Resistant Cell Line A549 and the Doxorubicin-Resistant Cell Line HEPG2

	IC_{50} [a] (μM)			IC_{50} [a] (μM)		
compd	A549	A549/CDDP	resistant factor[b]	HEPG2	HEPG2/DOX	resistant factor[b]
23a	0.009 ± 0.001	0.032 ± 0.009	3.56	0.006 ± 0.002	0.029 ± 0.004	4.83
25a	0.002 ± 0.002	0.009 ± 0.003	4.09	0.004 ± 0.001	0.008 ± 0.001111	2.00
25d	0.003 ± 0.001	0.011 ± 0.001	3.67	0.004 ± 0.002	0.005 ± 0.0012	1.25
CA4	0.004 ± 0.001	0.017 ± 0.003	4.25	0.009 ± 0.003	0.027 ± 0.006	3.00
EP128495	0.003 ± 0.001	0.009 ± 0.001	3.00	0.005 ± 0.002	0.011 ± 0.002	2.21
CDDP	8.917 ± 0.013	>10	nd	>10	>10	nd
DOX	2.905 ± 0.009	4.59 ± 0.063	1.58	1.89 ± 0.08	>10	nd

[a]Data are presented as the mean ± SE from the dose−response curves of at least three independent experiments. [b]Selectivity ratio = (IC_{50} human resistance cells)/(IC_{50} human cancer sensitive cells).

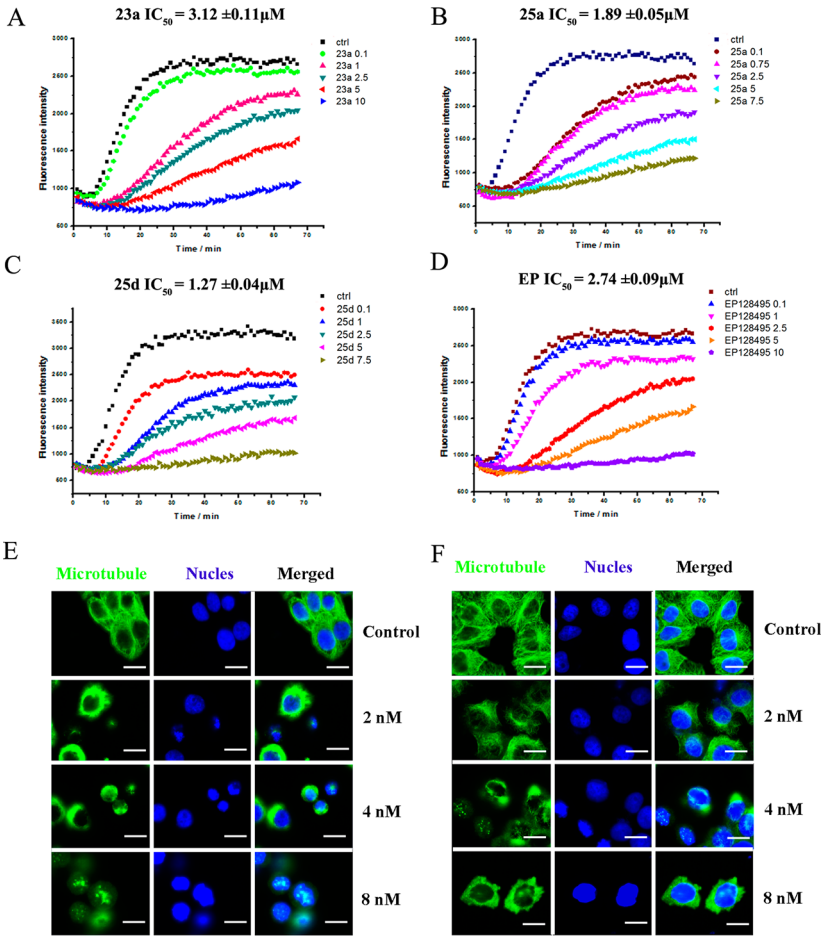

Figure 3. Effects on microtubule dynamics and microtubule network. Purified tubulin protein at 10 mM in a reaction buffer was incubated at 37 °C in the absence (control) or presence of **23a** (A), **25a** (B), **25d** (C), and EP128495 (D) at the indicated concentrations (ranging from 0.1 to 10 μM). And cultured A549 and HeLa cells were incubated in the presence of varying concentrations of compound **25a** for 12 h. The samples were stained for immunofluorescence using Alexa-Fluor 488 antibody (green) and corresponding Hoechst 33342 conjugated (blue). Images of the spindle microtubule in the control and treated A549 cells (E) and HeLa cells (F) were taken under LSM 570 laser confocal microscope. The results represent the best of data collected from three experiments with similar results (n = 3). Scale bars: 10 μm.

and **25d**, we used the cisplatin-resistant cell line A549/CDDP and the doxorubicin-resistant cell line HEPG2/DOX for an anti-MDR potential study, with EP128495 as the reference compound. The results in Table 4 indicated that **23a**, **25a**, and **25d** could effectively inhibit the proliferation of the cell lines A549/CDDP (IC_{50} values of 32, 9, and 11 nM; RF of 3.56, 4.09, and 3.67, respectively) and HEGP2/DOX (IC_{50} values of 29, 8, and 5 nM, RF of 4.83, 2.00, and 1.25, respectively) with very small resistant factor values. From the data it can be concluded that these selenium-containing compounds possess potent anti-MDR potential and deserve further study.

Inhibition of Microtubule Assembly and Induction of Morphological Aberrations. Tubulin is an essential eukaryotic protein that plays critical roles in cell division.[27] To investigate whether the activities of these selenium-containing 4-anilinoquinazoline derivatives were related to the interactions with microtubule systems, the most cytotoxic compounds **23a**, **25a**, **25d** and reference compounds EP128495

DOI: 10.1021/acs.jmedchem.8b00128
J. Med. Chem. XXXX, XXX, XXX−XXX

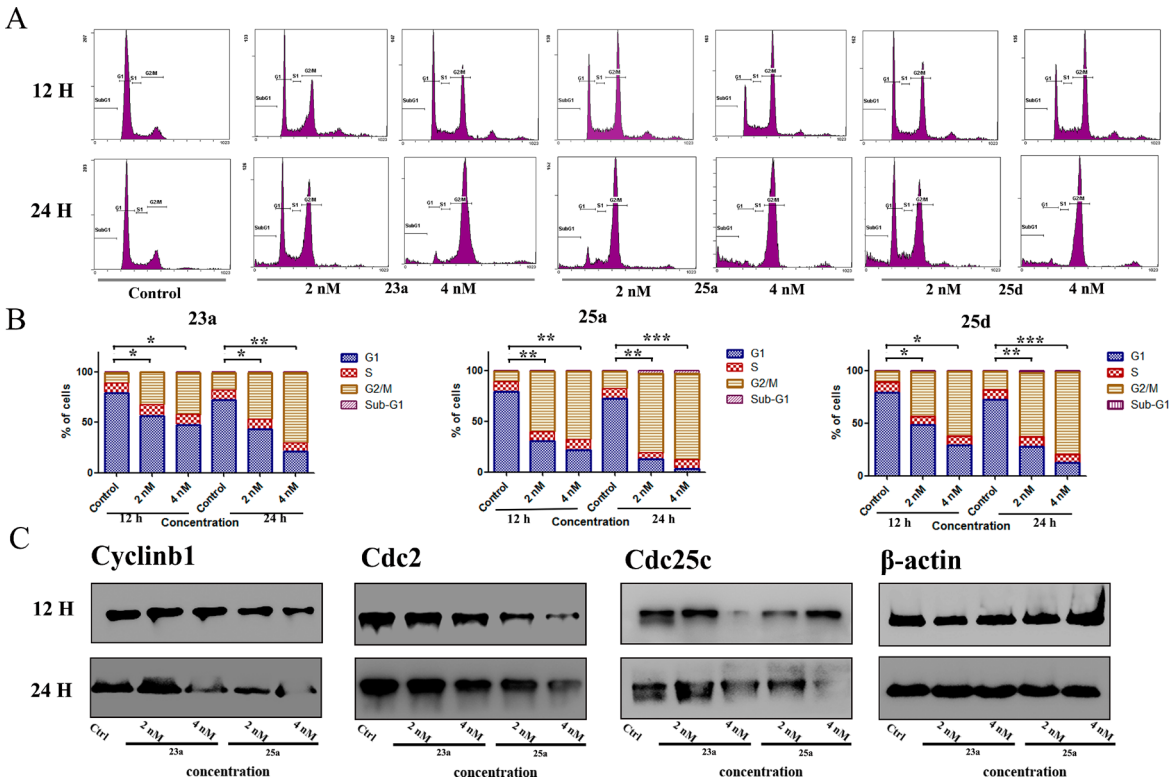

Figure 4. Effect of **23a**, **25a**, and **25d** on cell cycle progression. (A) A549 cells (3×10^5 cells/sample) were treated with increasing concentrations of **23a**, **25a**, and **25d** for 12 or 24 h. Cells were harvested, fixed with 70% ethanol, and stained with propidium iodide (PI). The cellular DNA content was then determined by flow cytometry analysis. (B) Quantitative analysis of the percentage of cells in each cell cycle phase was analyzed by EXPO32 ADC analysis software. (C) A549 cells were treated with **23a**, **25a**, and **25d** for various lengths of time, and whole-cell lysates were subjected to Western blotting using antibodies against the indicated proteins. The experiments were performed three times, and the results of representative experiments are shown: (*) $P < 0.05$, (**) $P < 0.01$, (***) $P < 0.001$ vs the control group.

were evaluated as tubulin polymerization inhibitors. The results indicated that **23a**, **25a**, and **25d** produced a concentration-dependent inhibition of tubulin polymerization, with calculated IC_{50} values of 3.12 ± 0.11 μM, 1.89 ± 0.05 μM, and 1.27 ± 0.04 μM, respectively (Figure 3A–C). Interestingly, **25d** exhibited the best tubulin polymerization inhibitory activity (90.46%) at a concentration of 7.5 μM, compared with 77.63% for the reference compound EP128495 (7.5 μM). Thus, the results indicated that compounds **23a**, **25a**, and **25d** might inhibit the cellular proliferation activity by direct inhibition of tubulin polymerization. Therefore, next we determined the effect of optimal compounds on the microtubule cytoskeleton of A549 and HeLa cells. After incubation for 12 h in the presence of **25a** or DMSO (0.01%), cells were surveyed with an LSM 570 laser confocal microscope. As shown in Figure 3, in the control, the integrity of the mitotic spindle and cellular microtubule network of the two cells were observed. After treatment with **25a** at a concentration of 2 nM, the spindle microtubule organization was not significantly deranged, but at the concentrations of 4 nM, the nucleus of the cells narrowed sharply and the spindle microtubules were completely disorganized. Furthermore, treatment with 8 nM compound **25a** led to a significant decrease in the polymeric tubulin fraction (Figure 3E,F).

Detection of Cell Cycle and Related Protein Expressions. In the following study, the most valid compounds **23a**, **25a**, and **25d** were examined for its effect on cell cycle progression of A549 cells by flow cytometry. Treatment of **23a**, **25a**, and **25d** (2 and 4 nM) for 12 or 24 h resulted in a gradual accumulation of cells in the G2/M phase of the cell cycle in a concentration-dependent manner, whereas the vehicle cells were primarily in the G1 phase (Figure 4A). Compound **23a** led to an accumulation of cells in the G2/M phase, from 10.13% (0.01% DMSO) to 69.69% (4 nM), with a concomitant decrease of cells in the G1 and S phase cells. This phenomenon is more obvious for compounds **25a** and **25d** at 4 nM for 12 h, which arrested 67.1% and 60.89% of the cells respectively in the G2/M phase, and when exposed to 4 nM for 24 h, the percentage of cells in the G2/M phase increased to 87.16% and 79.71%, respectively. These results implied that these compounds induce cell cycle arrest at the G2/M phase, probably through induction of apoptosis.

As karyokinesis, promoted by the factors Cdc25C, Cdc2, and cyclin B1, is an important event for eukaryotic cell entry into mitosis, we then investigated the correlation of **23a** and **25a**, which induced G2/M phase arrest, with alterations in the expression of proteins that regulate cell division. As depicted in Figure 4C, treatment with **23a** and **25a** resulted in dose- and time-dependent decreased expression of the Cdc25C, Cdc2, and cyclin B1 proteins. These results, which fit perfectly along with the results of cell cycle analysis described in Figure 4A, revealed that compounds **23a** and **25a** can convincingly induce G2/M phase arrest in A549 cells.

Detection of Apoptosis and Related Protein Expression. Mitotic arrest of tumor cells by tubulin-directed agents is generally associated with cellular apoptosis. To evaluate the capacity of compounds **23a**, **25a**, and **25d** to induce apoptosis in human cancer cell lines, a FITC conjugated annexin-V/PI

DOI: 10.1021/acs.jmedchem.8b00128
J. Med. Chem. XXXX, XXX, XXX–XXX

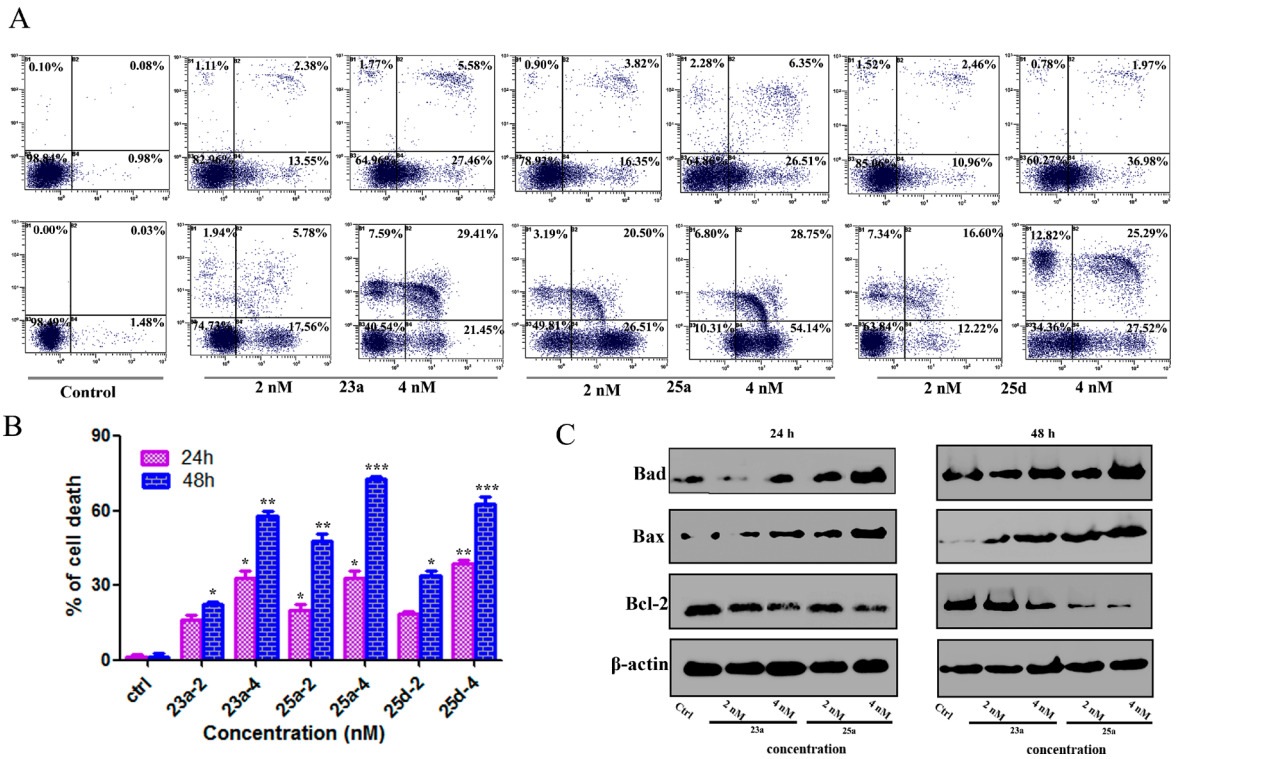

Figure 5. Inhibition of proliferation and induction of apoptosis in the cultured A549 cells upon treatment with compound **23a**, **25a**, and **25d**. (A) Dot plot representation of annexin-V-FITC fluorescence (*x*-axis) vs PI fluorescence (*y*-axis) of the apoptotic A549 (annexin-V positive) cells, treated with **23a**, **25a**, and **25d** (15, 10 nM) for 24 h and 48h. (B) Total apoptosis cells percentage were obtained by EXPO32 ADC analysis software. (C) Analysis of the expression of proteins cyclin B1, Cdc25c, and Cdc2 by Western blot. The experiments were performed three times, and the results of representative experiments are shown: (∗) $P < 0.05$, (∗∗) $P < 0.01$, (∗∗∗) $P < 0.001$ vs the control group.

assay was performed with A549 cells. As exhibited in Figure 5A, after A549 cells were exposed to 2 or 4 nM of the compounds **23a**, **25a**, and **25d** for 24 h, the total fractions of early apoptotic cells (annexin-V+/PI−) and late apoptotic cells (annexin-V +/PI+) were 15.93%, 20.17%, and 18.49%, respectively, for the concentration of 2 nM and were 33.04%, 37.17%, and 38.95% for 4 nM, compared with 1.06% for the control. After 48 h incubation, the percentages of early and late apoptotic cells strikingly increased to 22.34%, 47.86%, 39.97% (2 nM) and 57.86%, 72.89%, 64.71% (4 nM), respectively.

Increasing evidence has indicated that the regulation of the Bcl- 2 family of proteins is involved in the signaling pathways that are induced by antimicrotubule agents and are classified as either activators (e.g., Bax and Bad) or inhibitors (e.g., Bcl-2). As shown in Figure 5C, after treatment with compounds **23a** and **25a**, the level of Bax and Bad was efficiently up-regulated, whereas the antiapoptotic protein Bcl-2 was down-regulated significantly. Thus, as described above, compounds **23a**, **25a**, and **25d** exert excellent antiproliferative activity, display tubulin polymerization inhibition, and induce significant cell cycle arrest and cell apoptosis.

Effects on Mitochondrial Dysfunction and ROS Generation. Decreased mitochondrial membrane potential (MMP, $\Delta\Psi_m$) has been implicated as an early event in apoptotic cells. To confirm this property, we utilized a quantitative MMP assay to measure the activities of JC-1 stained mitochondria. As presented in Figure 6A, with the concentration of **25a** increasing from 2 nM to 8 nM, there is an obvious shift in JC-1 aggregates to increased forms of JC-1 monomers (the red fluorescence intensity decreased from 83.86% to 36.52%, and the green fluorescence intensity accordingly increased from 15.85% to 63.13%), which indicated that compound **25a** decreased the MMP of A549 cells during the apoptosis process. To further illustrate this phenomenon, a confocal microscopy assay was performed. The results in Figure 6B were consisted with that of flow cytometry and showed a shift toward the monomer form and a decrease of the aggregates.

Mitochondria are an important intracellular source of reactive oxygen species (ROS).[28−30] To further explore the mechanism of compound **25a** for inhibiting tumor cells, we measured the ability of compound **25a** to generate ROS in A549 cells using an oxidation-sensitive fluorescent probe (DCFH-DA). As the results illustrated in Figure 6D, the green fluorescence, which reflects the level of intracellular ROS, was difficult to observe in the control group. In contrast, after compound **25a** was added for 12 h, the intensity of the green fluorescence was brighter than that of the control group. Furthermore, the intensity of the green fluorescence became progressively brighter when the concentration of compound **25a** was increased. Altogether, according to the observed loss of mitochondrial potential, compound **25a** was able to increase ROS levels and eventually triggered apoptotic cell death.

Inhibition of A549 Cells Migration. Tumor cell migration is one of the important causes leading to the death of tumor patients. To determine the inhibitory ability of **23a**, **25a**, and **25d** to cell motility, A549 cells or PC9 cells (5×10^4 cells per well) were seeded in six-well plates and cultured as confluent monolayers. Figure 7 showed the typical images of the wound at the beginning of the experiment (0 h) and after 24 h of the control and the tested compounds (4 nM). It is obvious that the wound closure of the migration was significantly suppressed

DOI: 10.1021/acs.jmedchem.8b00128
J. Med. Chem. XXXX, XXX, XXX−XXX

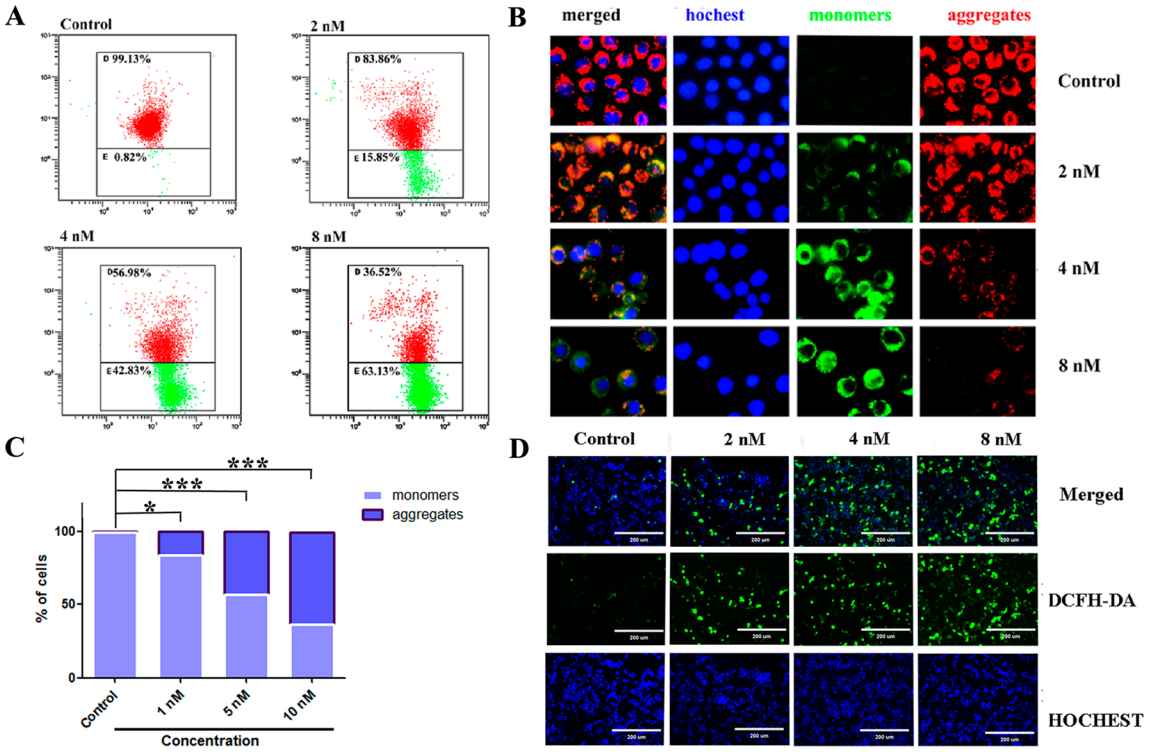

Figure 6. Decreased the mitochondrial membrane potential and increased ROS levels by **25a** of A549 cells. The A549 cells were treated with **25a** at different concentrations (2, 4, and 8 nM) or DMSO (0.01%) for 48 h, followed by incubation with the fluorescent probe JC-1 for 30 min. Then, the cells were analyzed by flow cytometry (A) or fluorescence microscopy (B). (D) The fluorescence images (magnification, 10× objective) demonstrate the motivation of **25a**-induced ROS. The experiments were performed at least three times, and the results of the representative experiments are shown.

for **23a**, **25a**, and **25d** treated groups compared to the control. Accordingly, the inhibition rate of migration was in the order of **25a** > **25d** > **23a** > EP128495 > control. Together these results indicated that **23a**, **25a**, and **25d** displayed an obvious inhibitory effect on migration of NSCLC cell and may be a promising candidate for chemotherapy of metastatic cancer.

Selectivity of 23a, 25a, and 25d toward Normal Cells. To study the selectivity of **23a**, **25a**, and **25d** for tumor cells and normal cells, four types of nontumorigenic cell lines from different origins, including human normal liver cells (LO2), human embryonic lung fibroblast cells (HLF), and human dermal fibroblast cells (BJ), were used for the test. The results in Table 5 showed that **23a**, **25a**, and **25d** are associated with a relatively low toxicity in nontumorigenic cell lines, which exhibited a 4.1-fold to 10-fold selectivity ratio for human nontumorigenic cells vs tumorigenic cells.

Antitumor Activity of Compounds 23a·HCl, 25a·HCl, and 25d·HCl in A549 Xenografts. To evaluate the antitumor potency of these selenium-containing 4-anilinoquinazoline derivatives in vivo, we established xenograft models by subcutaneously injecting A549 cells at the logarithmic growth phase into the right armpit of mice. Compounds **23a**, **25a**, and **25d** were selected for an in vivo xenografts mouse study in light of its nanomolar potency in vitro in the NCI cancer cell line panel and its potent depolymerization activity. EP128495·HCl and CA-4P were used as reference compounds. As the bioavailability of pharmacological agents largely depends on their water solubility, **23a**, **25a**, **25d**, and EP128495 were used in their hydrochloride forms. When the tumor sizes of well-established A549 xenografts were about 100 mm^3, the mice were randomly allocated to six groups (vehicle-treated, CA-4P-treated, EP128495·HCl-treated, **23a**·HCl-treated, **25a**·HCl-treated, and **25d**·HCl-treated groups), with 5 mice per group. After the acute toxicity experiment was performed, the safe dosage was determined. Then, the mice were intraperitoneally injected with CA-4P at a dose of 30 mg/kg and with compounds **23a**·HCl, **25a**·HCl, **25d**·HCl, and EP128495·HCl at a dose of 2.5 mg/kg every 2 days for the entire observation period. As shown in Figure 8A, treatment with compounds **23a**·HCl, **25a**·HCl, **25d**·HCl, EP128495·HCl, and CA-4P resulted in significant reductions, 69.85%, 75.69%, 77.23%, 68.62%, and 56.62%, respectively, in the tumor volume compared with the vehicle group.

CONCLUSION

Selenium is an essential trace mineral nutrient with multiple roles in the growth and function of living animal cells, and it effectively inhibits tumorigenesis in both animal models and epidemiological studies. In the present study, 28 novel selenium-containing 4-anilinoquinazoline derivatives were synthesized and evaluated for antiproliferative activity. The SAR indicated that 4-methylseleno derivatives exhibited greater potencies compared to that of other series (compounds **7**, **16**, and **23**). Especially, compounds **25a** and **25d** exhibited the most potent antiproliferative activities against six human cancer cell lines with IC_{50} values of 0.004−0.022 μM. Moreover, compounds **25a** and **25d** inhibited tubulin polymerization effectively and concentration-dependently with IC_{50} values of 1.89 ± 0.05 and 1.27 ± 0.04, respectively, which indicated that compounds **25a** and **25d** might inhibit cellular proliferative activity by direct inhibition of tubulin polymerization. Interestingly, compounds **25a** and **25d** also displayed equally

DOI: 10.1021/acs.jmedchem.8b00128
J. Med. Chem. XXXX, XXX, XXX−XXX

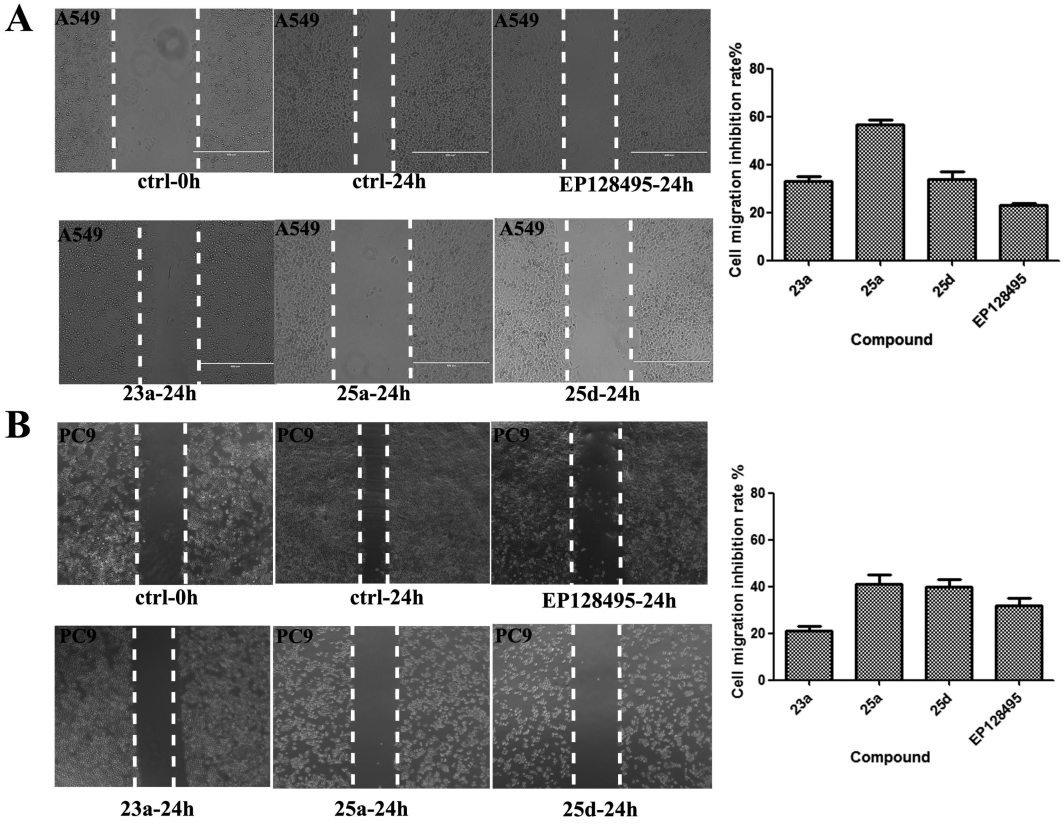

Figure 7. Effect of **23a**, **25a**, **25d**, and EP128495 on the migration of A549 or PC9 cells. A549 or PC9 cells (5×10^4 cells) suspended in free serum DMEM containing **23a**, **25a**, **25d**, and EP128495 (4 nM) for 24 h were photographed under a phase contrast microscopy (magnification, 4× objective). All results were expressed as the mean ± SD of at least three independent experiments.

Table 5. Antiproliferative Activity of Compounds 23a, 25a, and 25d against Human Normal Cells

	compd			
	23a	**25a**	**25d**	EP128495
Lo2, IC_{50} (μM)[a]	0.037 ± 0.009	0.019 ± 0.003	0.016 ± 0.001	0.013 ± 0.002
HLF, IC_{50} (μM)[a]	0.041 ± 0.011	0.020 ± 0.001	0.019 ± 0.001	0.018 ± 0.001
BJ, IC_{50} (μM)[a]	0.033 ± 0.009	0.019 ± 0.001	0.019 ± 0.001	0.015 ± 0.002
A549, IC_{50} (μM)[a]	0.009 ± 0.001	0.002 ± 0.002	0.002 ± 0.001	0.003 ± 0.001
resistant[b]	4.1/4.6/3.7	9.5/10/9.5	8/9.5/9.5	6.5/9/7.5

[a]Data are presented as the mean ± SE from the dose−response cures of at least three independent experiments. [b]Selectivity ratio = (IC50 human normal cells)/(IC50 A549).

potent cytotoxicity against several drug-resistant cell lines and showed high selectivity for normal human cells. Further flow cytometry analysis showed that **25a** and **25d** induce G2/M phase arrest and apoptosis in A549 cells. Cellular studies revealed that the induction of apoptosis by **25a** and **25d** was associated with a collapse of the mitochondrial membrane potential and alterations in the expression of some cell-cycle-related proteins (e.g., cyclin B1, Cdc25c, Cdc2) and apoptosis-related proteins (e.g., Bax, Bad, Bcl-2, Bcl-xl). In addition to these mechanism studies, we also evaluated the antitumor potency of compounds **23a**, **25a**, and **25d** in vivo. Treatment with these compounds resulted in a significant reduction in the tumor volume compared with the vehicle group, with 69.85%, 75.69%, and 77.23% tumor volume reductions observed, respectively. Taken together, these in vitro and in vivo results suggest that **25a** and **25d** may be promising lead compounds for the development of new anticancer drugs.

EXPERIMENTAL SECTION

General Methods (Chemistry). All reagents used in the synthesis were obtained commercially and used without further purification unless otherwise specified. The ^{1}H NMR and ^{13}C NMR spectra were recorded using TMS as the internal standard on a Bruker BioSpin GmbH spectrometer at 400 and 101 MHz, respectively. High-resolution mass spectra (HR-MS) were obtained using a Shimadzu LCMS-ITTOF mass spectrometer. The melting points were determined using an SRS-OptiMelt automated melting point instrument. The reactions were monitored by thin layer chromatography (TLC) on glass-packed precoated silica gel plates and visualized in an iodine chamber or with a UV lamp. Flash column chromatography was performed using silica gel (200−300 mesh) purchased from Qingdao Haiyang Chemical Co. Ltd. Chemicals and solvents were of reagent grade and used as obtained from Alfa Aesar (Ward Hill, MS) and Sigma-Aldrich (St. Louis, MO) without further purification. The purity of all the final synthesized compounds was ≥95% as determined by high-performance liquid chromatography (HPLC) with a TC-C18 column (4.6 mm × 250 mm, 5 μm).

DOI: 10.1021/acs.jmedchem.8b00128
J. Med. Chem. XXXX, XXX, XXX−XXX

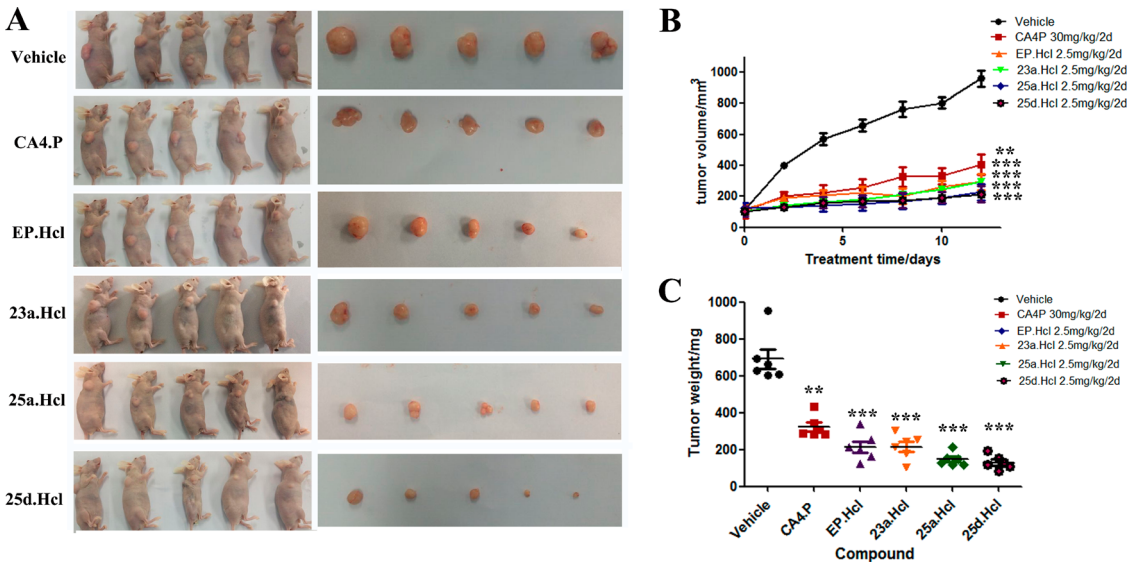

Figure 8. Antitumor activity in vivo. A549 cells were injected into the flanks of nude mice. When the tumor volume reached about 100 mm^3, the mice were sorted into six groups (n = 5) and administration started. (A) Images of sacrificed mice and excised tumors in each group. (B) Growth difference of tumor volumes. (C) At the end of experiment, tumors were resected and weighed. ● indicates the weight value of each tumor; the black line indicates the average value of the tumor weights.

Preparation of Intermediate 2. To a solution of 2-hydroxy-5-nitrobenzoic acid (5 mmol, 0.91 g) in 50 mL of acetone, K_2CO_3 (15 mmol, 2.07 g) was added. When the mixture was warmed to 60 °C, dimethyl sulfate (5 mmol, 0.63 g) was added in dropwise. The reaction was continued at the same temperature until the material disappeared as monitored by TLC. Water was added to the solution, and the mixture was then placed at room temperature for 2 h. The precipitates were collected to obtain the methyl 2-hydroxy-5-nitrobenzoate (91% yield). ^{1}H NMR (400 MHz, chloroform-d) δ 8.71 (d, J = 2.8 Hz, 1H), 8.37 (dd, J = 9.2, 2.9 Hz, 1H), 7.08 (d, J = 9.2 Hz, 1H), 4.03 (s, 4H), 3.94 (d, J = 1.1 Hz, 3H).

To a solution of methyl 2-hydroxy-5-nitrobenzoate (5 mmol, 0.985 g) in 20 mL of methanol, 100 mg of 10% Pd/C was added in batches. The reaction system was replaced by nitrogen three times and then hydrogenated with H_2 at room temperature and monitored by TLC. The catalyst was filtered and the solvent was removed in vacuum to afford an oily product for the use of next step without further purification (100%yield). MS (ESI) (m/z) $[M + H]^+$: 182.2.

Preparation of Intermediate 3. To a solution of intermediate **2** (2 mmol, 0.385 g) in 20 mL of water-free ethanol, paraformaldehyde (2 mmol, 0.18 g) and a drop of acetic acid as the catalyst were added. After the reaction was carried out for 2 h at room temperature, sodium cyanoborohydride (2 mmol, 0.126 g) was added and the reaction was continued until the material disappeared as monitored by TLC. The solvent was removed in vacuum, and 50 mL of ethanol was added to the mixture. The resulting mixture was washed by saturated sodium carbohydrate and water subsequently, dried over sodium sulfate, concentrated in vacuum to afford pale yellow oily intermediate **3** (78% yield). MS (ESI) (m/z) $[M + H]^+$: 196.1.

Preparation of Intermediate 4. To a solution of **3** (2 mmol, 0.392 g) in 20 mL of 2-propanol, 4-chloro-2-methylquinazoline (2 mmol, 0.357 g) was added at room temperature. After the reaction finished, 2-propanol was removed in vacuum and water was added to the residue. The resulting solution was adjusted to pH 9 by sodium carbonate and then extracted with ethyl acetate. The organic phase was washed with water, dried over sodium sulfate, concentrated, and purified by column chromatography to afford compound **4** (89% yield). ^{1}H NMR (400 MHz, DMSO-d_6) δ 7.68 (dd, J = 8.4, 1.3 Hz, 1H), 7.61 (ddd, J = 8.3, 6.7, 1.4 Hz, 1H), 7.52 (d, J = 2.8 Hz, 1H), 7.42 (dd, J = 8.9, 2.9 Hz, 1H), 7.19 (d, J = 8.9 Hz, 1H), 7.11 (ddd, J = 8.3, 6.7, 1.5 Hz, 1H), 7.00 (dd, J = 8.6, 1.3 Hz, 1H), 3.85 (s, 3H), 3.74 (s, 3H), 3.50 (s, 3H), 2.60 (s, 3H).

Preparation of Intermediate 5. To a solution of **4** (2 mmol, 0.675 g) in methanol and water (v/v = 1:1), sodium hydroxide (2 mmol, 0.08 g) was added. The reaction was constituted at room temperature until the materials disappeared as monitored by TLC. Methanol was removed in vacuum, and the solution was adjusted to pH 7 by saturated ammonium chloride, extracted with ethyl acetate for three times. The organic phase was washed with water, dried over sodium sulfate, concentrated to afford intermediate **5** (91.0% yield). MS (ESI) (m/z) $[M + H]^+$: 324.1.

Preparation of Intermediate 6a. Intermediate **5** (2 mmol, 0.646 g) was dissolved in 10 mL of $SOCl_2$, and the reaction system was heated at 80 °C for 2 h. The excess thionyl chloride was removed in vacuum, and the resulting acyl chloride was dissolved in 10 mL of dichloromethane. The acyl chloride solution obtained above was added dropwise to a solution of 2-bromoethan-1-amine (3 mmol) in 10 mL of dichloromethane at 0 °C and then reacted at room temperature. After the reaction finished (monitored by TLC), the reaction mixture was washed with saturated sodium carbonate and water, dried over sodium sulfate, concentrated, and purified by column chromatography to afford oily compound **6a** (75% yield). MS (ESI) (m/z) $[M + H]^+$: 429.2.

General Preparation of Intermediate 6b–f. To a solution of compound **5** (2 mmol, 0.646 g) in 20 mL of ancetonitrile, potassium carbonate (2 mmol) was added. After the mixture was stirred at room temperature for 15 min, dibromoethane or corresponding dibromoalkane (2 mmol) was added, and the reaction was stirred at reflux until the material disappeared. The solvent was removed in vacuum and the residue was dissolved in 20 mL of ethyl acetate, washed with water, dried over sodium sulfate, concentrated, and purified by column chromatography to afford oily compounds **6b–f**.

2-Bromoethyl 2-Methoxy-5-(methyl(2-methylquinazolin-4-yl)amino)benzoate (6b). Yellow oily liquid, 76.0% yield. ^{1}H NMR (400 MHz, chloroform-d) δ 7.76 (dt, J = 8.4, 0.9 Hz, 1H), 7.73 (d, J = 2.9 Hz, 1H), 7.55 (ddd, J = 8.4, 6.6, 1.7 Hz, 1H), 7.20 (dd, J = 8.9, 2.9 Hz, 1H), 7.08–6.98 (m, 2H), 6.94 (d, J = 8.9 Hz, 1H), 4.58 (t, J = 6.2 Hz, 2H), 3.93 (s, 3H), 3.60 (m, 5H), 2.74 (s, 3H).

3-Bromopropyl 2-Methoxy-5-(methyl(2-methylquinazolin-4-yl)amino)benzoate (6c). Yellow oily liquid, 74.0% yield. ^{1}H NMR (400 MHz, chloroform-d) δ 7.76 (d, J = 8.4 Hz, 1H), 7.66 (d, J = 2.8 Hz, 1H), 7.58–7.52 (m, 1H), 7.20 (dt, J = 8.8, 3.2 Hz, 1H), 7.08–6.97 (m, 2H), 6.94 (d, J = 8.9 Hz, 1H), 4.42 (t, J = 6.0 Hz, 2H), 3.92 (s, 3H), 3.60 (s, 3H), 2.73 (s, 3H), 2.26 (p, J = 6.2 Hz, 2H), 1.89–1.78 (m, 2H).

DOI: 10.1021/acs.jmedchem.8b00128
J. Med. Chem. XXXX, XXX, XXX–XXX

4-Bromobutyl 2-Methoxy-5-(methyl(2-methylquinazolin-4-yl)amino)benzoate (6d). Yellow oily liquid, 76.0% yield. ^{1}H NMR (400 MHz, chloroform-*d*) δ 7.80−7.73 (m, 1H), 7.66 (d, *J* = 2.9 Hz, 1H), 7.55 (ddd, *J* = 8.4, 6.5, 1.7 Hz, 1H), 7.20 (dd, *J* = 8.8, 2.9 Hz, 1H), 7.07−6.97 (m, 2H), 6.94 (d, *J* = 8.9 Hz, 1H), 4.31 (t, *J* = 6.1 Hz, 2H), 3.92 (s, 3H), 3.60 (s, 3H), 3.44 (t, *J* = 6.5 Hz, 2H), 2.73 (s, 3H), 2.08−1.81 (m, 4H).

5-Bromopentyl 2-Methoxy-5-(methyl(2-methylquinazolin-4-yl)amino)benzoate (6e). Yellow oily liquid, 73.0% yield. ^{1}H NMR (400 MHz, chloroform-*d*) δ 7.76 (d, *J* = 8.4 Hz, 1H), 7.67 (d, *J* = 2.8 Hz, 1H), 7.55 (ddd, *J* = 8.2, 6.5, 1.7 Hz, 1H), 7.20 (dd, *J* = 8.9, 2.8 Hz, 1H), 7.08−6.97 (m, 2H), 6.94 (d, *J* = 8.8 Hz, 1H), 4.29 (t, *J* = 6.5 Hz, 2H), 3.93 (s, 3H), 3.60 (s, 3H), 3.42 (q, *J* = 6.5 Hz, 2H), 2.73 (s, 3H), 1.88 (ddd, *J* = 18.3, 12.8, 6.9 Hz, 2H), 1.74 (h, *J* = 8.2, 7.3 Hz, 2H), 1.56 (ddt, *J* = 15.1, 10.4, 6.3 Hz, 2H).

6-Bromohexyl 2-Methoxy-5-(methyl(2-methylquinazolin-4-yl)amino)benzoate (6f). Yellow oily liquid, 75.0% yield. ^{1}H NMR (400 MHz, chloroform-*d*) δ 7.76 (d, *J* = 8.4 Hz, 1H), 7.66 (d, *J* = 2.8 Hz, 1H), 7.55 (ddd, *J* = 8.4, 6.5, 1.7 Hz, 1H), 7.19 (dd, *J* = 8.8, 2.9 Hz, 1H), 7.07−6.96 (m, 2H), 6.94 (d, *J* = 8.9 Hz, 1H), 4.28 (t, *J* = 6.6 Hz, 2H), 3.92 (s, 3H), 3.60 (s, 3H), 3.40 (t, *J* = 6.7 Hz, 2H), 2.73 (s, 3H), 1.86 (p, *J* = 6.9 Hz, 2H), 1.75 (dq, *J* = 14.1, 7.2 Hz, 2H), 1.46 (dp, *J* = 23.0, 7.7, 7.3 Hz, 4H).

General Synthesis of Target Compounds 7a−f. To a solution of **6a** (or **6b−f**) (1 mmol) in 5 mL of acetonitrile, KSeCN (1.5 mmol) was added, and the mixture was stirred at reflux until the reaction finished. Ethyl acetate 20 mL of was added and the mixture was washed with saturated sodium carbonate and water, dried over sodium sulfate, concentrated, and purified by column chromatography to afford oily compounds **7a−f**.

2-Methoxy-5-(methyl(2-methylquinazolin-4-yl)amino)-*N*-(2-selenocyanatoethyl)benzamide (7a). Yellow oily liquid, 76.0% yield. ^{1}H NMR (400 MHz, chloroform-*d*) δ 8.45 (t, *J* = 6.0 Hz, 1H), 8.17 (d, *J* = 3.0 Hz, 1H), 7.74 (d, *J* = 8.4 Hz, 1H), 7.52 (ddd, *J* = 8.4, 6.5, 1.7 Hz, 1H), 7.11 (dd, *J* = 8.8, 3.0 Hz, 1H), 7.04−6.94 (m, 2H), 6.92 (d, *J* = 8.8 Hz, 1H), 3.99 (s, 3H), 3.92 (q, *J* = 6.3 Hz, 2H), 3.59 (s, 3H), 3.35 (t, *J* = 6.3 Hz, 2H), 2.72 (s, 3H). ^{13}C NMR (101 MHz, chloroform-*d*) δ 165.05, 163.28, 161.72, 155.63, 151.89, 142.37, 131.87, 130.41, 129.40, 127.61, 126.01, 124.25, 122.13, 114.57, 112.82, 101.42, 56.50, 42.44, 40.33, 29.13, 26.31. HRMS (ESI) *m*/*z* [M + H]$^+$ for $C_{21}H_{21}N_5O_2Se$ pred 456.0934, meas 456.0948.

2-Selenocyanatoethyl 2-Methoxy-5-(methyl(2-methylquinazolin-4-yl)amino)benzoate (7b). Yellow oily liquid, 75.0% yield. ^{1}H NMR (400 MHz, chloroform-*d*) δ 7.80−7.71 (m, 2H), 7.55 (ddd, *J* = 8.4, 6.5, 1.7 Hz, 1H), 7.23 (dd, *J* = 8.9, 2.8 Hz, 1H), 7.11−6.98 (m, 2H), 6.95 (d, *J* = 8.9 Hz, 1H), 4.66 (t, *J* = 6.1 Hz, 2H), 3.94 (s, 3H), 3.60 (s, 3H), 3.38 (t, *J* = 6.2 Hz, 2H), 2.73 (s, 3H). ^{13}C NMR (101 MHz, chloroform-*d*) δ 164.66, 163.39, 161.64, 157.53, 152.18, 141.24, 131.90, 131.48, 129.21, 127.84, 125.98, 124.31, 120.00, 114.54, 113.41, 100.76, 63.26, 56.32, 42.45, 27.31, 26.47. HRMS (ESI) *m*/*z* [M + H]$^+$ for $C_{21}H_{21}N_4O_3Se$ pred 457.0775, meas 457.0781.

3-Selenocyanatopropyl 2-Methoxy-5-(methyl(2-methylquinazolin-4-yl)amino)benzoate (7c). Yellow oily liquid, 72.0% yield. ^{1}H NMR (400 MHz, chloroform-*d*) δ 7.79−7.72 (m, 1H), 7.63 (d, *J* = 2.8 Hz, 1H), 7.55 (ddd, *J* = 8.4, 6.4, 1.9 Hz, 1H), 7.25 (dd, *J* = 8.9, 2.8 Hz, 1H), 7.06−6.99 (m, 2H), 6.96 (d, *J* = 8.9 Hz, 1H), 4.41 (t, *J* = 5.8 Hz, 2H), 3.92 (s, 3H), 3.60 (s, 3H), 3.12 (t, *J* = 7.1 Hz, 2H), 2.73 (s, 3H), 2.37−2.27 (m, 2H). ^{13}C NMR (101 MHz, chloroform-*d*) δ 165.21, 163.39, 161.63, 157.17, 152.15, 141.23, 131.88, 131.02, 128.87, 127.84, 125.95, 124.25, 120.86, 114.53, 113.43, 101.17, 63.15, 56.31, 42.43, 29.83, 26.41, 25.96. HRMS (ESI) *m*/*z* [M + H]$^+$ for $C_{22}H_{22}N_4O_3Se$ pred 471.0931, meas 471.0930.

4-Selenocyanatobutyl 2-Methoxy-5-(methyl(2-methylquinazolin-4-yl)amino)benzoate (7d). Yellow oily liquid, 73.0% yield. ^{1}H NMR (400 MHz, chloroform-*d*) δ 7.76 (dt, *J* = 8.4, 1.0 Hz, 1H), 7.65 (d, *J* = 2.9 Hz, 1H), 7.54 (ddd, *J* = 8.4, 6.5, 1.8 Hz, 1H), 7.22 (dd, *J* = 8.8, 2.9 Hz, 1H), 7.08−6.97 (m, 2H), 6.95 (d, *J* = 8.9 Hz, 1H), 4.32 (t, *J* = 6.2 Hz, 2H), 3.93 (s, 3H), 3.60 (s, 3H), 3.08 (t, *J* = 7.2 Hz, 2H), 2.73 (s, 3H), 2.10−1.99 (m, 2H), 1.95−1.83 (m, 2H). ^{13}C NMR (101 MHz, chloroform-*d*) δ 165.39, 163.37, 161.62, 157.18, 152.13, 141.18, 131.86, 130.87, 128.90, 127.78, 125.97, 124.26, 121.30, 114.54, 113.40, 101.07, 63.96, 56.31, 42.47, 28.87, 28.09, 27.67, 26.40. HRMS (ESI) *m*/*z* [M + H]$^+$ for $C_{23}H_{24}N_4O_3Se$ pred 485.1088, meas 485.1090.

5-Selenocyanatopentyl 2-Methoxy-5-(methyl(2-methylquinazolin-4-yl)amino)benzoate (7e). Yellow oily liquid, 71.0% yield. ^{1}H NMR (400 MHz, chloroform-*d*) δ 7.76 (d, *J* = 8.4 Hz, 1H), 7.64 (d, *J* = 2.7 Hz, 1H), 7.55 (ddd, *J* = 8.3, 6.6, 1.7 Hz, 1H), 7.23 (dd, *J* = 9.0, 2.8 Hz, 1H), 7.07−7.00 (m, 2H), 6.96 (d, *J* = 8.8 Hz, 1H), 4.29 (t, *J* = 6.4 Hz, 2H), 3.93 (s, 3H), 3.60 (s, 3H), 3.03 (t, *J* = 7.4 Hz, 2H), 2.73 (s, 3H), 1.94 (p, *J* = 7.3 Hz, 2H), 1.76 (h, *J* = 8.0, 7.4 Hz, 2H), 1.53 (ddd, *J* = 15.0, 8.8, 6.5 Hz, 2H). ^{13}C NMR (101 MHz, chloroform-*d*) δ 165.30, 163.37, 161.60, 157.24, 152.11, 141.08, 131.88, 130.82, 128.88, 127.76, 126.00, 124.27, 121.41, 114.53, 113.39, 101.33, 64.58, 56.31, 42.51, 30.39, 29.24, 27.88, 26.45, 25.58.

6-Selenocyanatohexyl 2-Methoxy-5-(methyl(2-methylquinazolin-4-yl)amino)benzoate (7f). Yellow oily liquid, 71.0% yield. ^{1}H NMR (400 MHz, chloroform-*d*) δ 7.78−7.73 (m, 1H), 7.64 (d, *J* = 2.8 Hz, 1H), 7.54 (ddd, *J* = 8.4, 6.6, 1.7 Hz, 1H), 7.21 (dd, *J* = 8.8, 2.9 Hz, 1H), 7.06−6.97 (m, 2H), 6.95 (d, *J* = 8.9 Hz, 1H), 4.27 (t, *J* = 6.6 Hz, 2H), 3.92 (s, 3H), 3.60 (s, 3H), 3.03 (t, *J* = 7.3 Hz, 2H), 2.73 (s, 3H), 1.90 (p, *J* = 7.3 Hz, 2H), 1.80−1.68 (m, 2H), 1.55−1.37 (m, 4H). ^{13}C NMR (101 MHz, chloroform-*d*) δ 165.37, 163.34, 161.59, 157.20, 152.14, 141.09, 131.83, 130.70, 128.82, 127.78, 125.98, 124.23, 121.65, 114.54, 113.42, 101.35, 64.82, 56.30, 42.47, 30.70, 29.34, 28.65, 28.36, 26.42, 25.23. HRMS (ESI) *m*/*z* [M + H]$^+$ for $C_{25}H_{28}N_4O_3Se$ pred 513.1401, meas 513.1420.

Preparation of the Intermediate 8. Sodium (25 mmol) was added to 100 mL of methanol at 0 °C. After the reaction finished, 4-fluoro-3-nitroaniline (5 mmol, 0.78 g) was added, and then the mixture was refluxed until the reaction finished. Paraformaldehyde (5 mmol, 0.45 g) was added when reaction system was cooled to room temperature. After the mixture was stirred at room temperature for 2 h, sodium borohydride (5 mmol, 0.185 g) was added, and the mixture was stirred at reflux. After the reaction finished (monitored by TLC), the solvent was removed in vacuum and water was added. The mixture was extracted three times with ethyl acetate, washed with ammonium chloride and then water, dried over sodium sulfate, concentrated, and purified by column chromatography to give compound **8** (77% yield). Yellow solid. ^{1}H NMR (400 MHz, DMSO-d_6) δ 8.08 (s, 1H), 7.50 (s, 1H), 7.30 (d, *J* = 9.4 Hz, 1H), 7.00 (d, *J* = 9.4 Hz, 1H), 3.75 (s, 3H), 2.95 (s, 3H).

Preparation of the Intermediate 9. To a solution of **8** (2 mmol, 0.364 g) in 20 mL of 2-propanol, 4-chloro-2-methylquinazoline (2 mmol, 0.358 g) was added, and the mixture was stirred at room temperature. After the reaction finished (monitored by TLC), 2-propanol was removed in vacuum and the resulting solid was dissolved in 20 mL of methanol. To the solution above, 40 mg of 10% Pd/C was added in batches. The reaction system was replaced by nitrogen three times and then hydrogenated with H_2 at room temperature and monitored by TLC. The catalyst were filtered and the solvent was removed in vacuum to afford the intermediate **9** (100% yield). Yellow solid. ^{1}H NMR (400 MHz, chloroform-*d*) δ 7.74−7.68 (m, 1H), 7.51 (ddd, *J* = 8.4, 6.9, 1.4 Hz, 1H), 7.14 (dd, *J* = 8.6, 1.4 Hz, 1H), 6.98 (ddd, *J* = 8.5, 6.9, 1.3 Hz, 1H), 6.73 (d, *J* = 8.4 Hz, 1H), 6.57 (d, *J* = 2.5 Hz, 1H), 6.51 (dd, *J* = 8.4, 2.6 Hz, 1H), 3.88 (s, 3H), 3.87 (s, 2H), 3.56 (s, 3H), 2.70 (s, 3H).

Preparation of Target Compound 10. To a solution of intermediate **9** (2 mmol, 0.689 g) in 25 mL of water containing 0.5 mL of concentrated hydrogen chloride at 0 °C, sodium nitrite (2 mmol) was added slowly. After the reaction was continued for 30 min, the solution was adjusted to pH 6 by sodium acetate and then KSeCN (2 mmol) was added in batches. The mixture was stirred at room temperature until the reaction finished monitored by TLC. Ethyl acetate (50 mL) was added and the organic phase was washed with sodium carbonate and water subsequently, dried over sodium sulfate, concentrated, and purified by column chromatography to give compound **10** (50% yield). Yellow solid. ^{1}H NMR (400 MHz, chloroform-*d*) δ 7.79 (d, *J* = 8.5 Hz, 1H), 7.60 (d, *J* = 2.5 Hz, 1H), 7.59−7.52 (m, 1H), 7.04 (d, *J* = 3.6 Hz, 2H), 6.99 (dd, *J* = 8.7, 2.5 Hz,

DOI: 10.1021/acs.jmedchem.8b00128
J. Med. Chem. XXXX, XXX, XXX−XXX

1H), 6.81 (d, J = 8.7 Hz, 1H), 3.91 (s, 3H), 3.61 (s, 3H), 2.74 (s, 3H). ^{13}C NMR (101 MHz, chloroform-d) δ 163.31, 161.60, 153.91, 151.86, 143.64, 132.02, 127.67, 127.40, 127.25, 125.82, 124.42, 114.49, 114.39, 111.60, 100.86, 56.63, 42.70, 26.25. HRMS (ESI) m/z [M + H]$^+$ for $C_{18}H_{16}N_4OSe$ pred 385.0563, meas 385.0566.

Preparation of the Intermediate 12. To a solution of 2-methoxy-5-nitrophenol (5 mmol, 0.85 g) in 50 mL of dry dichloromethane, DIPEA (7.5 mmol) was added at 0 °C. After the mixture was stirred for 5 min, methyl chloromethyl ether (6 mmol) was added slowly and the reaction was continued at the same temperature until the starting materials disappeared. The mixture was washed with saturated ammonium chloride and water subsequently, dried over sodium sulfate, concentrated, and purified by column chromatography to give the intermediate 1-methoxy-2-(methoxymethoxy)-4-nitrobenzene as yellow solid (92% yield). ^{1}H NMR (400 MHz, DMSO-d_6) δ 7.97 (d, J = 8.9 Hz, 1H), 7.90 (s, 1H), 7.23 (d, J = 9.0 Hz, 1H), 5.30 (s, 2H), 3.93 (s, 3H), 3.41 (s, 3H).

Intermediate 1-methoxy-2-(methoxymethoxy)-4-nitrobenzene (4 mmol, 0.85 g) was dissolved in 20 mL of methanol, and 80 mg of 10% Pd/C was added in batches. The reaction system was replaced by nitrogen three times and then hydrogenated with H_2 at room temperature and monitored by TLC. The catalyst was filtered and the solvent was removed in vacuum to afford the intermediate **12** (100% yield) as pale yellow liquid. ^{1}H NMR (400 MHz, chloroform-d) δ 6.73 (d, J = 8.5 Hz, 1H), 6.60 (d, J = 2.6 Hz, 1H), 6.31 (dd, J = 8.5, 2.7 Hz, 1H), 5.19 (s, 2H), 3.80 (s, 3H), 3.51 (s, 3H).

Preparation of the Intermediate 13. Sodium (10 mmol, 0.23 g) was added in 50 mL of methanol in 0 °C. After the metal dissolved completely, intermediate **12** (2 mmol, 0.43 g) and paraformaldehyde (2 mmol) were added. After the mixture was stirred at room temperature for two hours, sodium borohydride (2 mmol, 0.076 g) was added and the reaction was stirred at 60 °C until it finished. The solvent was removed in vacuum, and then water and ethyl acetate were added to the residue. The organic phase was washed with saturated ammonium chloride and water subsequently, dried over sodium sulfate, concentrated, and purified by column chromatography to give the intermediate **13** (77% yield) as yellow liquid. ^{1}H NMR (400 MHz, chloroform-d) δ 6.79 (d, J = 8.6 Hz, 1H), 6.53 (d, J = 2.6 Hz, 1H), 6.23 (dd, J = 8.7, 2.7 Hz, 1H), 5.20 (s, 2H), 3.80 (s, 3H), 3.51 (s, 3H), 2.79 (s, 3H).

Preparation of the Intermediate 14. To a solution of 4-chloro-2-methylquinazoline in 20 mL of 2-propanol, intermediate **13** (2 mmol, 0.366 g) was added, and the mixture was stirred at room temperature until the reaction finished. Solvent was removed in vacuum, and the residue was dissolved in 50 mL of saturated HCl methanol. After the mixture was stirred at room temperature for 0.5 h, the solution was adjusted to pH 9, extracted with ethyl acetate three times, washed with water, dried over sodium sulfate, concentrated, and purified by column chromatography to give the intermediate **14** (89% yield) as white liquid. ^{1}H NMR (400 MHz, DMSO-d_6) δ 9.74 (s, 1H), 7.92 (d, J = 8.4 Hz, 1H), 7.86 (t, J = 7.7 Hz, 1H), 7.31 (t, J = 7.9 Hz, 1H), 7.09 (d, J = 8.5 Hz, 1H), 6.94 (s, 1H), 6.90 (d, J = 8.6 Hz, 1H), 6.86 (d, J = 8.8 Hz, 1H), 3.85 (s, 3H), 3.71 (s, 3H), 2.75 (s, 3H).

General Preparation of the Intermediates 15a–e. To a solution of intermediate **14** (2 mmol, 0.59 g) in 20 mL of acetonitrile, potassium carbonate (4 mmol) was added. After the mixture was stirred for 15 min at room temperature, dibromoethane or corresponding dibromoalkane (2 mmol) was added and the reaction was stirred at reflux until the material disappeared. The solvent was removed in vacuum and the residue was dissolved in 20 mL of ethyl acetate, washed with water, dried over sodium sulfate, concentrated, and purified by column chromatography to afford the intermeadiates **15a–e**.

***N*-(3-(2-Bromoethoxy)-4-methoxyphenyl)-*N*,2-dimethylquinazolin-4-amine (15a).** ^{1}H NMR (400 MHz, chloroform-d) δ 7.78–7.71 (m, 1H), 7.53 (ddd, J = 8.4, 6.7, 1.6 Hz, 1H), 7.08–6.95 (m, 2H), 6.87 (d, J = 8.6 Hz, 1H), 6.80 (dd, J = 8.5, 2.5 Hz, 1H), 6.73 (d, J = 2.5 Hz, 1H), 4.21 (t, J = 6.5 Hz, 2H), 3.90 (s, 3H), 3.59 (s, 3H), 3.56 (t, J = 6.5 Hz, 2H), 2.72 (s, 3H).

***N*-(3-(3-Bromopropoxy)-4-methoxyphenyl)-*N*,2-dimethylquinazolin-4-amine (15b).** ^{1}H NMR (400 MHz, chloroform-d) δ 7.73 (d, J = 8.3 Hz, 1H), 7.52 (ddd, J = 8.3, 6.8, 1.5 Hz, 1H), 7.04 (dd, J = 8.5, 1.3 Hz, 1H), 6.98 (ddd, J = 8.5, 6.8, 1.3 Hz, 1H), 6.85 (d, J = 8.5 Hz, 1H), 6.79–6.71 (m, 2H), 4.02 (t, J = 5.9 Hz, 2H), 3.89 (s, 3H), 3.60 (s, 3H), 3.56 (t, J = 6.4 Hz, 2H), 2.72 (s, 3H), 2.27 (p, J = 6.2 Hz, 2H).

***N*-(3-(4-Bromobutoxy)-4-methoxyphenyl)-*N*,2-dimethylquinazolin-4-amine (15c).** ^{1}H NMR (400 MHz, chloroform-d) δ 7.73 (d, J = 8.3 Hz, 1H), 7.58–7.45 (m, 1H), 7.04 (d, J = 9.0 Hz, 1H), 7.00–6.93 (m, 1H), 6.86 (d, J = 8.5 Hz, 1H), 6.76 (dd, J = 8.5, 2.4 Hz, 1H), 6.68 (d, J = 2.4 Hz, 1H), 3.90 (d, J = 7.9 Hz, 5H), 3.59 (s, 3H), 3.44 (t, J = 6.6 Hz, 2H), 2.72 (s, 3H), 2.00 (q, J = 6.9 Hz, 2H), 1.94–1.87 (m, 2H).

***N*-(3-(5-Bromopentyloxy)-4-methoxyphenyl)-*N*,2-dimethylquinazolin-4-amine (15d).** ^{1}H NMR (400 MHz, chloroform-d) δ 7.73 (d, J = 8.4 Hz, 1H), 7.53 (ddd, J = 8.3, 6.7, 1.5 Hz, 1H), 7.03 (dd, J = 8.5, 1.4 Hz, 1H), 6.97 (ddd, J = 8.4, 6.7, 1.3 Hz, 1H), 6.85 (d, J = 8.5 Hz, 1H), 6.75 (dd, J = 8.5, 2.4 Hz, 1H), 6.67 (d, J = 2.5 Hz, 1H), 3.89 (d, J = 5.1 Hz, 5H), 3.60 (s, 3H), 3.40 (t, J = 6.8 Hz, 2H), 2.72 (s, 3H), 1.88 (p, J = 6.9 Hz, 2H), 1.76 (q, J = 6.9 Hz, 2H), 1.56 (tt, J = 9.8, 6.1 Hz, 2H).

***N*-(3-(6-Bromohexyloxy)-4-methoxyphenyl)-*N*,2-dimethylquinazolin-4-amine (15e).** ^{1}H NMR (400 MHz, chloroform-d) δ 7.73 (d, J = 8.3 Hz, 1H), 7.52 (t, J = 6.7 Hz, 1H), 7.03 (d, J = 8.5 Hz, 1H), 7.00–6.93 (m, 1H), 6.85 (d, J = 8.5 Hz, 1H), 6.75 (d, J = 8.6 Hz, 1H), 6.67 (s, 1H), 3.95–3.81 (m, 5H), 3.59 (d, J = 1.5 Hz, 3H), 3.40 (d, J = 6.8 Hz, 2H), 2.72 (d, J = 1.4 Hz, 3H), 1.85 (t, J = 6.9 Hz, 2H), 1.74 (d, J = 7.6 Hz, 2H), 1.50–1.38 (m, 4H).

General Preparation of the Target Products 16a–e. To a solution of **15a–e** (1 mmol) in 5 mL of acetonitrile, KSeCN (1.5 mmol) was added, and the mixture was stirred at reflux. After the reaction finished (monitored by TLC), ethyl acetate (20 mL) was added. The mixture was washed with saturated sodium carbonate and water, dried over sodium sulfate, concentrated, and purified by column chromatography to give the target products **16a–e**.

***N*-(4-Methoxy-3-(2-selenocyanatoethoxy)phenyl)-*N*,2-dimethylquinazolin-4-amine (16a).** ^{1}H NMR (400 MHz, chloroform-d) δ 7.74 (d, J = 6.9 Hz, 1H), 7.53 (ddd, J = 8.3, 6.5, 1.8 Hz, 1H), 7.06–6.95 (m, 2H), 6.88 (d, J = 8.6 Hz, 1H), 6.83 (dd, J = 8.6, 2.5 Hz, 1H), 6.72 (d, J = 2.5 Hz, 1H), 4.29 (t, J = 6.2 Hz, 2H), 3.89 (s, 3H), 3.59 (s, 3H), 3.32 (t, J = 6.1 Hz, 2H), 2.72 (s, 3H). ^{13}C NMR (101 MHz, chloroform-d) δ 163.37, 161.55, 152.12, 148.50, 147.90, 141.75, 131.78, 127.73, 126.02, 124.05, 120.09, 114.65, 113.57, 112.95, 101.01, 68.27, 56.13, 42.52, 27.85, 26.45. HRMS (ESI) m/z [M + H]$^+$ for $C_{20}H_{20}N_4O_2Se$ pred 429.0825, meas 429.0834.

***N*-(4-Methoxy-3-(3-selenocyanatopropoxy)phenyl)-*N*,2-dimethylquinazolin-4-amine (16b).** ^{1}H NMR (400 MHz, chloroform-d) δ 7.74 (d, J = 8.4 Hz, 1H), 7.53 (ddd, J = 8.4, 6.6, 1.7 Hz, 1H), 7.03 (ddd, J = 8.5, 1.6, 0.6 Hz, 1H), 7.01–6.96 (m, 1H), 6.86 (d, J = 8.6 Hz, 1H), 6.79 (dd, J = 8.5, 2.4 Hz, 1H), 6.69 (d, J = 2.5 Hz, 1H), 4.00 (t, J = 5.6 Hz, 2H), 3.88 (s, 3H), 3.59 (s, 3H), 3.25 (t, J = 6.8 Hz, 2H), 2.72 (s, 3H), 2.32 (p, J = 6.8 Hz, 2H). ^{13}C NMR (101 MHz, chloroform-d) δ 163.33, 161.51, 152.04, 148.61, 148.19, 141.64, 131.74, 127.64, 126.06, 124.01, 119.19, 114.66, 112.51, 112.15, 101.80, 67.53, 56.03, 42.57, 29.98, 26.43, 26.26. HRMS (ESI) m/z [M + H]$^+$ for $C_{21}H_{22}N_4O_2Se$ pred 443.0982, meas 443.0975.

***N*-(4-Methoxy-3-(4-selenocyanatobutoxy)phenyl)-*N*,2-dimethylquinazolin-4-amine (16c).** ^{1}H NMR (400 MHz, chloroform-d) δ 7.73 (d, J = 8.3 Hz, 1H), 7.52 (ddd, J = 8.3, 6.6, 1.5 Hz, 1H), 7.03 (dd, J = 8.5, 1.4 Hz, 1H), 7.01–6.94 (m, 1H), 6.85 (d, J = 8.5 Hz, 1H), 6.76 (dd, J = 8.5, 2.4 Hz, 1H), 6.67 (d, J = 2.4 Hz, 1H), 3.92 (t, J = 6.0 Hz, 2H), 3.87 (s, 3H), 3.59 (s, 3H), 3.11 (t, J = 7.2 Hz, 2H), 2.71 (s, 3H), 2.05 (q, J = 7.2 Hz, 2H), 1.89 (q, J = 6.1 Hz, 2H). ^{13}C NMR (101 MHz, chloroform-d) δ 163.24, 161.43, 151.90, 148.90, 148.02, 141.48, 131.72, 127.48, 126.14, 124.00, 118.61, 114.62, 112.29, 111.42, 101.63, 68.27, 56.03, 42.62, 29.44, 28.04, 27.81, 26.42. HRMS (ESI) m/z [M + H] + for $C_{22}H_{24}N_4O_2Se$ pred 457.1138, meas 457.1148.

***N*-(4-Methoxy-3-(5-selenocyanatopentyloxy)phenyl)-*N*,2-dimethylquinazolin-4-amine (16d).** ^{1}H NMR (400 MHz, chloroform-d) δ 7.73 (d, J = 8.3 Hz, 1H), 7.58–7.47 (m, 1H), 7.06–6.93 (m,

DOI: 10.1021/acs.jmedchem.8b00128
J. Med. Chem. XXXX, XXX, XXX–XXX

2H), 6.85 (d, J = 8.5 Hz, 1H), 6.75 (dd, J = 8.5, 2.4 Hz, 1H), 6.67 (d, J = 2.5 Hz, 1H), 3.92−3.83 (m, 5H), 3.59 (s, 3H), 3.02 (t, J = 7.4 Hz, 2H), 2.71 (s, 3H), 1.91 (p, J = 7.4 Hz, 2H), 1.77 (p, J = 6.7 Hz, 2H), 1.56 (qd, J = 9.3, 8.8, 6.1 Hz, 2H). 13C NMR (101 MHz, chloroform-d) δ 163.24, 161.42, 151.90, 149.10, 148.04, 141.46, 131.71, 127.46, 126.17, 123.98, 118.40, 114.62, 112.31, 111.37, 101.51, 68.53, 56.09, 42.62, 30.53, 29.25, 28.12, 26.44, 25.61. HRMS (ESI) m/z [M + H] + for $C_{23}H_{26}N_4O_2Se$ pred 471.1295, meas 471.1309.

***N*-(4-Methoxy-3-(6-selenocyanatohexyloxy)phenyl)-*N*,2-dimethylquinazolin-4-amine (16e).** ^{1}H NMR (400 MHz, chloroform-d) δ 7.73 (d, J = 8.4 Hz, 1H), 7.52 (t, J = 7.2 Hz, 1H), 7.03 (d, J = 8.5 Hz, 1H), 6.97 (t, J = 7.2 Hz, 1H), 6.86 (d, J = 8.5 Hz, 1H), 6.76 (dd, J = 8.5, 2.3 Hz, 1H), 6.67 (s, 1H), 3.94−3.83 (m, 5H), 3.60 (s, 3H), 3.04 (t, J = 7.4 Hz, 2H), 2.72 (s, 3H), 1.90 (p, J = 6.8 Hz, 2H), 1.76 (t, J = 6.8 Hz, 2H), 1.52−1.39 (m, 4H). ^{13}C NMR (101 MHz, chloroform-d) δ 163.31, 161.47, 151.92, 149.26, 148.05, 141.50, 131.74, 127.47, 126.19, 124.01, 118.30, 114.67, 112.27, 111.29, 101.49, 68.71, 56.13, 42.65, 30.66, 29.41, 28.75, 28.67, 26.43, 25.21. HRMS (ESI) m/z $[M + H]^+$ for $C_{24}H_{28}N_4O_2Se$ pred 485.1452, meas 485.1452.

Preparation of the Intermediate 17. To a tetrahydrofuran solution (25 mL), lithium aluminum hydride (10 mmol) was added at 0 °C, and then intermediate **4** (2 mmol, 0.675 g) in 10 mL of tetrahydrofuran was added in dropwise. The reaction mixture was warmed to room temperature and monitored by TLC. After the reaction finished, ice−water was added to quench the reaction and then sodium sulfate. After the mixture was stirred for 30 min, the mixture was filtrated and the residue was washed with ethyl acetate for three times. The combined organic phase was concentrated and purified by column chromatography to give the intermediate **17** (45.0% yield). ^{1}H NMR (400 MHz, DMSO-d_6) δ 7.88−7.80 (m, 2H), 7.48 (d, J = 2.8 Hz, 1H), 7.35 (dd, J = 8.6, 2.8 Hz, 1H), 7.31−7.24 (m, 1H), 7.12 (d, J = 8.7 Hz, 1H), 6.80 (d, J = 8.7 Hz, 1H), 4.52 (s, 2H), 3.86 (s, 3H), 3.74 (s, 3H), 2.74 (s, 3H).

Preparation of the Target Compound 19. Intermediate **17** (2 mmol, 0.618 g) was dissolved in 10 mL of thionyl chloride, and the mixture was stirred at reflux for 2 h. The excess thionyl chloride was removed under vacuum, and the residue was dissolved in 10 mL of acetonitrile. Potassium selenocyanate (3 mmol) was added, and then the mixture was heated to reflux. After the reaction finished, ethyl acetate (50 mL) was added and the organic phase was washed with saturate sodium carbonate, dried over sodium sulfate, and purified by column chromatography to give the **19** (40.0% yield). ^{1}H NMR (400 MHz, chloroform-d) δ 7.75 (dd, J = 8.4, 1.3 Hz, 1H), 7.53 (ddd, J = 8.3, 6.5, 1.7 Hz, 1H), 7.18 (d, J = 2.7 Hz, 1H), 7.09−6.97 (m, 3H), 6.85 (d, J = 8.7 Hz, 1H), 4.21 (s, 2H), 3.91 (s, 3H), 3.59 (s, 3H), 2.73 (s, 3H). ^{13}C NMR (101 MHz, chloroform-d) δ 163.25, 161.64, 155.39, 151.86, 141.48, 131.87, 127.81, 127.54, 126.23, 126.09, 124.28, 114.56, 111.85, 102.07, 55.83, 42.53, 27.61, 26.36.

Preparation of the Intermediate 21. Sodium metal (10 mmol, 0.23 g) was added to 50 mL of anhydrous methanol. After the sodium dissolved completely, corresponding anilines (2 mmol) and paraformaldehyde (2 mmol) were added. The mixture was stirred at room temperature for 2 h, and then sodium borohydride (2 mmol) was added. The reaction was heated at 60 °C until the anilines disappeared. The solvent was removed, and water and ethyl acetate were added to the residue. The organic phase was separated and the water phase was extracted by ethyl acetate. The combined organic phase was washed by saturated ammonium chloride and water, dried over sodium sulfate, concentrated, and purified by column chromatography to give the intermediatea **21a−d** in 93−96% yields.

General Preparation of the Intermediates 22a−d. To a solution of malononitrile (2 mmol) in 15 mL of dimethyl sulfoxide, selenium dioxide (2 mmol) was added at 0 °C. After the mixture was stirred for 5 min, the reaction was warmed to room temperature and the stirred for another 15 min. Intermediate **21a** or **21b−d** were added to the mixture, and the reaction was continued until finished (monitored by TLC). Water was added to the reaction system and extracted by ethyl acetate three times. The combined organic phase was washed by brine and then water, dried over sodium sulfate, concentrated, and purified by column chromatography to give the intermediates **22a−d**.

***N*-Methyl-4-selenocyanatoaniline (22a).** Pale yellow solid (76.0% yield). ^{1}H NMR (400 MHz, chloroform-d) δ 7.47 (d, J = 8.5 Hz, 2H), 6.55 (d, J = 8.4 Hz, 2H), 2.84 (s, 3H).

***N*,3-Dimethyl-4-selenocyanatoaniline (22b).** Pale yellow solid (78.0% yield). ^{1}H NMR (400 MHz, chloroform-d) δ 7.48 (d, J = 8.5 Hz, 1H), 6.52 (s, 1H), 6.38 (d, J = 8.5 Hz, 1H), 2.83 (s, 3H), 2.49 (s, 3H).

3-Chloro-*N*-methyl-4-selenocyanatoaniline (22c). Pale yellow solid (75.0% yield). ^{1}H NMR (400 MHz, chloroform-d) δ 7.49 (d, J = 8.0 Hz, 1H), 6.46 (m, 2H), 2.83 (s, 3H).

3-Fluoro-*N*-methyl-4-selenocyanatoaniline (22d). Pale yellow solid (77.0% yield). ^{1}H NMR (400 MHz, chloroform-d) δ 7.41 (d, J = 7.9 Hz, 1H), 6.36 (m, 2H), 2.84 (s, 3H).

General Preparation of Target Compounds 23a−f. To a solution of 4-chloro-2-methylquinazoline (2 mmol) or 4-chloro-2-(methyl-d_3)quinazolinein, 25 mL of 2-propanol, intermediate **22a**, or **22b−d** was added, and the mixture was stirred at room temperature. After the reaction finished, 2-propanol was removed in vacuum, water was added. The solution was adjusted to pH 9 by saturated sodium carbonate, extracted with ethyl acetate three times. The combined organic phase was washed with water, dried over sodium sulfate, concentrated, and purified by column chromatography to give the intermediates **23a−f**.

***N*,2-Dimethyl-*N*-(4-selenocyanatophenyl)quinazolin-4-amine (23a).** Yellow solid (88% yield). ^{1}H NMR (400 MHz, chloroform-d) δ 7.81 (d, J = 8.4 Hz, 1H), 7.67−7.51 (m, 3H), 7.18−7.04 (m, 4H), 3.65 (s, 3H), 2.76 (s, 3H). ^{13}C NMR (101 MHz, chloroform-d) δ 163.57, 162.13, 152.24, 150.39, 134.71, 132.40, 128.07, 125.91, 124.88, 116.93, 115.03, 101.38, 41.66, 26.42. HRMS (ESI) m/z $[M + H]^+$ for $C_{17}H_{14}N_4Se$ pred 355.0457, meas 355.0448.

***N*,2-Dimethyl-*N*-(3-methyl-4-selenocyanatophenyl)-quinazolin-4-amine (23b).** Yellow solid (88% yield). ^{1}H NMR (400 MHz, chloroform-d) δ 7.80 (d, J = 8.4 Hz, 1H), 7.69−7.55 (m, 2H), 7.17−7.05 (m, 3H), 6.96−6.87 (m, 1H), 3.64 (s, 3H), 2.76 (s, 3H), 2.44 (s, 3H). ^{13}C NMR (101 MHz, chloroform-d) δ 163.55, 162.10, 152.19, 150.88, 142.26, 135.93, 132.34, 127.99, 126.73, 125.81, 118.44, 115.08, 100.98, 41.76, 26.43, 22.69. HRMS (ESI) m/z $[M + H]^+$ for $C_{18}H_{16}N_4Se$ pred 369.0614, meas 369.0610.

***N*,2-Dimethyl-*N*-(4-selenocyanatophenyl)quinazolin-4-amine (23c).** Yellow solid (89% yield). ^{1}H NMR (400 MHz, chloroform-d) δ 7.82 (d, J = 8.4 Hz, 1H), 7.63 (d, J = 8.2 Hz, 2H), 7.23−7.11 (m, 3H), 6.99 (d, J = 8.7, 1H), 3.63 (s, 3H), 2.75 (s, 3H). ^{13}C NMR (101 MHz, chloroform-d) δ 163.68, 162.08, 152.38, 150.63, 134.20, 132.69, 132.50, 128.27, 125.49, 125.28, 124.85, 124.10, 118.59, 115.13, 100.68, 41.60, 26.40. HRMS (ESI) m/z $[M + H]^+$ for $C_{17}H_{13}N_4ClSe$ pred 389.0065, meas 389.0046.

***N*,2-Dimethyl-*N*-(4-selenocyanatophenyl)quinazolin-4-amine (23d).** Yellow solid (90% yield). ^{1}H NMR (400 MHz, chloroform-d) δ 7.92−7.79 (m, 1H), 7.68 (ddd, J = 8.4, 6.8, 1.5 Hz, 1H), 7.57 (dd, J = 8.5, 7.5 Hz, 1H), 7.28 (dd, J = 8.3, 1.6 Hz, 1H), 7.21 (ddd, J = 8.3, 6.8, 1.2 Hz, 1H), 6.87 (ddd, J = 17.0, 9.2, 2.4 Hz, 2H), 3.67 (s, 3H), 2.79 (s, 3H). ^{13}C NMR (101 MHz, chloroform-d) δ 163.81, 162.39, 161.37 (d, J = 248.5 Hz), 152.49 (d, J = 9.4 Hz), 152.46, 135.35 (d, J = 2.8 Hz), 132.87, 128.32, 125.49, 125.42, 120.30 (d, J = 2.9 Hz), 115.52, 110.82 (d, J = 24.8 Hz), 102.80 (d, J = 22.5 Hz), 99.82 (d, J = 2.1 Hz), 41.27, 26.39. HRMS (ESI) m/z [M + H] + for $C_{17}H_{13}N_4FSe$ pred 373.0363, meas 373.0354.

***N*,2-Dimethyl-*N*-(4-selenocyanatophenyl)quinazolin-4-amine, 2-Methyl D3 (23e).** Yellow solid (85% yield). ^{1}H NMR (400 MHz, chloroform-d) δ 7.80 (dd, J = 8.6, 4.1 Hz, 1H), 7.58 (m, 3H), 7.20−6.99 (m, 4H), 3.70−3.57 (m, 3H). ^{13}C NMR (101 MHz, chloroform-d) δ 163.47, 162.09, 152.24, 150.35, 134.66, 132.35, 128.06, 125.87, 125.72, 124.85, 116.94, 115.03, 101.34, 41.62, 25.7 (m, CD_3). HRMS (ESI) m/z [M + H] + for $C_{17}H_{11}D_3N_4Se$ Se pred 358.0650, meas 358.0635.

2-Cyclopropyl-*N*-methyl-*N*-(4-selenocyanatophenyl)-quinazolin-4-amine (23f). Yellow solid (82% yield). ^{1}H NMR (400 MHz, chloroform-d) δ 7.78 (d, J = 8.4 Hz, 1H), 7.59−7.51 (m, 3H),

DOI: 10.1021/acs.jmedchem.8b00128
J. Med. Chem. XXXX, XXX, XXX−XXX

7.12−6.99 (m, 4H), 3.57 (d, J = 1.0 Hz, 3H), 2.35−2.21 (m, 1H), 1.30−1.21 (m, 2H), 1.05 (dq, J = 7.0, 3.8 Hz, 2H). ^{13}C NMR (101 MHz, chloroform-d) δ 167.18, 162.03, 152.27, 150.37, 134.66, 132.32, 127.85, 126.06, 125.77, 124.29, 116.97, 115.29, 101.45, 41.57, 18.43, 9.92. HRMS (ESI) m/z [M + H]$^+$ for $C_{19}H_{16}N_4Se$ pred 381.0614, meas 381.0612.

General Preparation of Target Compounds 25a−f. Compound **23a** (1 mmol) or **23b−g** were dissolved in 10 mL of absolute ethyl alcohol. Sodium borohydride (1 mmol) was added in batches to the solution and then methyl iodide (1.5 mmol). The reaction was stirred at room temperature until the starting material disappeared. Ammonium hydroxide (1 mL) was added to remove the excess methyl iodide, and the solvents were removed in vacuum. Water was added to the residue, and the mixture was extracted with ethyl acetate three times. The combined organic phase was washed with water, dried over sodium sulfate, concentrated, and purified by column chromatography to give the intermediates **25a−f**.

***N*,2-Dimethyl-*N*-(4-(methylselanyl)phenyl)quinazolin-4-amine (25a).** Yellow solid (88% yield). ^{1}H NMR (400 MHz, chloroform-d) δ 7.76 (d, J = 8.4 Hz, 1H), 7.53 (t, J = 8.2 Hz, 1H), 7.41−7.34 (m, 2H), 7.08 (d, J = 8.6 Hz, 1H), 7.06−6.97 (m, 3H), 3.59 (s, 3H), 2.73 (s, 3H), 2.35 (s, 3H). ^{13}C NMR (101 MHz, chloroform-d) δ 163.38, 161.76, 152.10, 146.86, 131.87, 131.56, 129.27, 127.75, 126.13 (d, J = 2.0 Hz), 124.22, 114.76, 42.20, 26.49, 7.40. HRMS (ESI) m/z [M + H]$^+$ for $C_{17}H_{17}N_3Se$ pred 344.0661, meas 344.0652.

***N*,2-Dimethyl-*N*-(3-methyl-4-(methylselanyl)phenyl)-quinazolin-4-amine (25b).** Yellow solid (90% yield). ^{1}H NMR (400 MHz, chloroform-d) δ 7.75 (dd, J = 8.5, 1.3 Hz, 1H), 7.52 (d, J = 8.4 Hz, 1H), 7.23 (d, J = 8.3 Hz, 1H), 7.09 (dd, J = 8.6, 1.5 Hz, 1H), 7.02−6.94 (m, 2H), 6.89 (dd, J = 8.3, 2.5 Hz, 1H), 3.59 (s, 3H), 2.73 (s, 3H), 2.31 (d, J = 2.0 Hz, 6H). ^{13}C NMR (101 MHz, chloroform-d) δ 163.37, 161.71, 152.10, 146.54, 139.56, 131.78, 130.49, 129.65, 127.68, 126.82, 126.20, 124.11, 123.76, 114.86, 42.31, 26.48, 21.77, 6.43. HRMS (ESI) m/z [M + H]$^+$ for $C_{18}H_{19}$N3Se pred 358.0818, meas 358.0809.

***N*-(3-Chloro-4-(methylselanyl)phenyl)-*N*,2-dimethyl-quinazolin-4-amine (25c).** Yellow solid (85% yield). ^{1}H NMR (400 MHz, chloroform-d) δ 7.78 (d, J = 8.4 Hz, 1H), 7.57 (d, J = 8.4 Hz, 1H), 7.22−7.12 (m, 3H), 7.07 (d, J = 8.3 Hz, 1H), 6.92 (dd, J = 8.5, 2.4 Hz, 1H), 3.59 (s, 3H), 2.74 (s, 3H), 2.33 (s, 3H). ^{13}C NMR (101 MHz, chloroform-d) δ 163.44, 161.74, 152.19, 147.32, 134.78, 132.11, 129.75, 129.56, 127.93, 125.89, 124.59, 124.21, 114.81, 42.10, 26.44, 6.55. HRMS (ESI) m/z [M + H]$^+$ for $C_{17}H_{16}ClN_3Se$ pred 378.0269, meas 378.0264.

***N*-(3-Fluoro-4-(methylselanyl)phenyl)-*N*,2-dimethyl-quinazolin-4-amine (25d).** Yellow solid (87% yield). ^{1}H NMR (400 MHz, chloroform-d) δ 7.79 (d, J = 8.5 Hz, 1H), 7.58 (d, J = 8.4 Hz, 1H), 7.35−7.24 (m, 1H), 7.17 (d, J = 8.6 Hz, 1H), 7.08 (d, J = 8.3 Hz, 1H), 6.86 (dd, J = 10.0, 2.3 Hz, 1H), 6.81 (dd, J = 8.3, 2.3 Hz, 1H), 3.61 (s, 3H), 2.75 (s, 3H), 2.34 (s, 3H). ^{13}C NMR (101 MHz, chloroform-d) δ 163.49, 161.93, 161.69 (d, J = 244.7 Hz), 152.23, 148.79 (d, J = 9.1 Hz), 132.48 (d, J = 5.0 Hz), 132.16, 127.97, 125.84, 124.62, 121.28 (d, J = 3.0 Hz), 115.25 (d, J = 22.7 Hz), 114.98, 112.08 (d, J = 24.8 Hz), 41.91, 26.44, 6.49 (d, J = 3.2 Hz). HRMS (ESI) m/z [M + H]$^+$ for $C_{17}H_{16}FN_3Se$ pred 362.0567, meas 362.0554.

***N*,2-Dimethyl-*N*-(4-(methylselanyl)phenyl)quinazolin-4-amine, 2-Methyl D3 (25e).** Yellow solid (89% yield). ^{1}H NMR (400 MHz, chloroform-d) δ 7.75 (d, J = 8.4 Hz, 1H), 7.52 (d, J = 6.9 Hz, 1H), 7.36 (d, J = 8.5 Hz, 2H), 7.08 (d, J = 8.6 Hz, 1H), 7.02 (m, 3H), 3.58 (d, J = 1.8 Hz, 3H), 2.34 (d, J = 1.8 Hz, 3H). ^{13}C NMR (101 MHz, chloroform-d) δ 163.30, 16.74, 152.08, 146.86, 131.83, 131.60, 129.27, 127.74, 126.10 (d, J = 2.1 Hz), 124.19, 114.78, 42.16, 28.23−24.09 (m,CD_3), 7.38. HRMS (ESI) m/z [M + H]$^+$ for $C_{17}H_{13}D_3N_3Se$ pred 347.0865, meas 347.0842.

2-Cyclopropyl-*N*-methyl-*N*-(4-(methylselanyl)phenyl)-quinazolin-4-amine (25f). Yellow solid (91% yield). ^{1}H NMR (400 MHz, chloroform-d) δ 7.73 (d, J = 8.4 Hz, 1H), 7.50 (t, J = 7.2 Hz, 1H), 7.35 (d, J = 10.3 Hz, 2H), 7.09−6.98 (m, 3H), 6.93 (d, J = 8.3 Hz, 1H), 3.52 (s, 3H), 2.34 (s, 3H). ^{13}C NMR (101 MHz, chloroform-d) δ 166.94, 161.69, 152.14, 146.86, 131.80, 131.54, 129.23, 127.56, 126.22, 126.11, 123.68, 115.11, 42.07, 18.40, 9.63, 7.40. HRMS (ESI) m/z [M + H]$^+$ for $C_{19}H_{19}N_3Se$ pred 370.0818, meas 370.0810.

Biology. Cell Lines and Culture. The human cancer cell lines (A549, HCT116, HEPG2, MDAMB231, LOVO, RKO, HELA, MCF7, MGC803, PC9, HLF, BJ, LO2, A549/CDDP, HEPG2/DOX) used in this study were purchased from the Laboratory Animal Service Center at Sun Yat-sen University (Guangzhou, China). Cell lines HELA, HEPG2, RKO, LOVO, MGC803, MCF7, MDAMB231, HLF, BJ, and LO2 were cultivated in DMEM containing 10% (v/v) heat-inactivated fetal bovine serum (FBS), 100 units/mL penicillin, and 100 μg/mL streptomycin. Cell lines A549, PC9, HCT116, HEPG2/DOX, and A549/CDDP were cultivated in RPMI 1640 medium containing 10% (v/v) heat-inactivated FBS, 100 units/mL penicillin, and 100 mg/mL streptomycin.

Antibodies and Reagents. A commercial kit (Cytoskeleton, catalog no. B011P) used for the tubulin polymerization assay was purchased from Cytoskeleton (Danvers, MA, USA). The FITC-conjugated mouse anti-tubulin antibody was purchased from Cell Signaling Technology (Danvers, MA, USA). The goat anti-mouse IgG/Alexa-Fluor 488 antibody was obtained from Invitrogen (Camarillo, CA, USA). A purified brain tubulin polymerization kit was purchased from Cytoskeleton (Danvers, MA, Q9 USA). Annexin-V/FITC and the cell cycle analysis kit were purchased from Keygen Biotech, China. MTT was purchased from Sigma, USA. A lipophilic cationic dye, 5,50,6,60-tetrachloro-1,10,3,30-tetraethylbenzimidazolcarbocyanine (JC-1), was obtained from Beyotime, China. The mouse anti-Bcl-xl monoclonal antibody, mouse anti-α-tubulin monoclonal antibody, rabbit anti-Bax, rabbit anti-Bad, rabbit anti-Bcl-2, rabbit anti-cyclin B1, rabbit anti-Cdc2, rabbit anti-Cdc25C, mouse anti-β-tubulin, and horseradish peroxidase-conjugated goat anti-mouse IgG secondary antibody were all obtained from Cell Signaling Technology (Danvers, MA, USA).

MTT Assay. For cytotoxicity assay, the cells grown in the logarithmic phase were seeded into 96-well plates (5×10^3 cells/well) for 24 h and then exposed to different concentrations of the test compounds for 48 h. After attached cells were incubated with 5 mg/mL MTT (Sigma, USA) for another 4 h, the suspension was discarded and subsequently the dark blue crystals (formazan) were dissolved in dimethyl sulfoxide (DMSO). Then the absorbance at 570 nm was measured using a multifunction microplate reader (Molecular Devices, Flex Station 3), and each experiment was performed at least in triplicate. The cytotoxic effects of each compound were expressed as IC_{50} values, which represent the drug concentrations required to cause 50% tumor cell growth inhibition, and calculated with GraphPad Prism software version 5.02 (GraphPad Inc., La Jolla, CA, USA).

In Vitro Tubulin Polymerization Assay and Immunofluorescence Microscopy. The tubulin polymerization assay was performed according to the method described by Bonne et al. with appropriate modification. The tubulin polymerization was monitored by an increase in fluorescence intensity, which can be easily recorded due to the incorporation of a fluorescent reporter, DAPI (4′,6-diamidino-2-phenylindole), a fluorophore already known as a DNA intercalator. We performed the tubulin polymerization assay using a commercial kit (Cytoskeleton, catalog no. BK011P) purchased from Cytoskeleton (Danvers, MA, USA). The final buffer concentration used for tubulin polymerization contained 80.0 mM piperazine-*N*,*N*′-bis(2-ethanesulfonic acid)sequisodium salt (pH 6.9), 2.0 mM $MgCl_2$, 0.5 mM EGTA, 1 mM GTP, and 10.2% glycerol. After 5 μL of the tested compounds at the indicated concentrations was added, the mixture was warmed to 37 °C for 1 min, and the reaction was initiated by the addition of 55 μL of the tubulin solution. The fluorescence intensity enhancement was recorded every 60 s for 90 min in a multifunction microplate reader (Molecular Devices, Flex Station 3) (emission wavelength is 410 nm; excitation wavelength is 340 nm). The area under the curve was used to determine the concentration that inhibited tubulin polymerization by 50% (IC_{50}), which was calculated with GraphPad Prism software version 5.02 (GraphPad Inc., La Jolla, CA, USA). For the immunofluorescence microscopy, 3×10^5 cells were grown in a 10 mm^3 confocal culture dish for 24 h and then incubated in the presence or absence of compound **25a** at the

DOI: 10.1021/acs.jmedchem.8b00128
J. Med. Chem. XXXX, XXX, XXX−XXX

indicated concentrations for another 12 h. After being washed with phosphate buffered solution (PBS) and fixed in 4% prewarmed (37 °C) paraformaldehyde for 15 min, the cells were permeabilized with 0.5% Triton X-100 for 15 min and blocked for 30 min in 10% goat serum. Then, the cells were incubated with mouse anti-tubulin antibody (CST, USA) at 4 °C overnight. On the next day, cells were washed with PBS three times and incubated with goat anti-mouse IgG/Alexa-Fluor 488 antibody (Invitrogen, USA) for 1 h. After the nuclei were stained with Hoechst 33342 (Sigma, USA) in the dark at room temperature for 30 min, the samples were immediately visualized on a Zeiss LSM 570 laser scanning confocal microscope (Carl Zeiss, Germany).

Cell Cycle Analysis. A549 cells were seeded in six-well plates (3×10^5 cells/well) and incubated in the presence or absence of compounds **23a**, **25a**, and **25d** at the indicated concentrations for 24 or 48 h. Then, cells were harvested by centrifugation and fixed in ice-cold 70% ethanol overnight. After the ethanol was removed on the next day, the cells were resuspended in the ice-cold PBS and treated with RNase A (Keygen Biotech, China) at 37 °C for 30 min, followed by incubation with the DNA staining solution propidium iodide (PI) (Keygen Biotech, China) at 4 °C for 30 min. About 10 000 events were detected by flow cytometry (Beckman Coulter, Epics XL) at 488 nm. The data regarding the number of cells in different phases of the cell cycle were analyzed by EXPO32 ADC analysis software.

Apoptosis Analysis. A549 cells were seeded in six-well plates (3×10^5 cells/well) and incubated in the presence or absence of compounds **23a**, **25a**, and **25d** at the indicated concentrations for 24 or 48 h to induce cell apoptosis. After incubation, cells were harvested and incubated with 5 μL of annexin-V/FITC (Keygen Biotech, China) in binding buffer (10 mM HEPES, 140 mM NaCl, and 2.5 mM $CaCl_2$ at pH 7.4) at room temperature for 15 min. PI solution was then added to the medium for another 10 min incubation. Almost 10 000 events were collected for each sample and analyzed by flow cytometry (Beckman Coulter, Epics XL). The percentage of apoptotic cells was calculated with EXPO32 ADC analysis software.

Western Blot Analysis. A549 cells seeded in 60 mm dishes at a density of 5×10^5 cells/well were incubated with or without compounds **23a**, **25a**, and **25d** at indicated concentrations for 24 or 48 h. After incubation, the cells were washed twice with ice-cold PBS and then lysed in RIPA lysis buffer containing 150 mM NaCl, 50 mM Tris (pH 7.4), 1% (w/v) sodium deoxycholate, 1% (v/v) Triton X-100, 0.1% (w/v) SDS, and 1 mM EDTA (Beyotime, China). The lysates were incubated at 0 °C for 30 min and vortexed every 10 min intermittently, and then the total protein was harvested by centrifuging at 12 500*g* for 15 min. After the protein concentrations were determined by a BCA protein assay kit (Thermo Fisher Scientific, Rockford, IL, USA), the protein extracts were reconstituted in loading buffer containing 62 mM Tris-HCl, 2% SDS, 10% glycerol, and 5% β-mercaptoethanol (Beyotime, China) and boiled at 100 °C for 3 min. An equal amount of the proteins (40 μg) was separated by 8−12% sodium dodecyl sulfate−polyacrylamide gel electrophoresis (SDS−PAGE) and transferred to nitrocellulose membranes (Amersham Biosciences, Little Chalfont, Buckinghamshire, U.K.). After blocked with 5% nonfat dried milk in TBS containing 1% Tween-20 for 90 min at room temperature, the membrane was incubated overnight with specific primary antibodies (CST, USA) at 4 °C. After three washes in TBST, the membranes were incubated with the appropriate HRP-conjugated secondary antibodies at room temperature for 2 h. The blots were developed with enhanced chemiluminescence (Pierce, Rockford, IL, USA) and were detected by an LAS4000 imager (GE Healthcare, Waukesha, WI, USA).

Mitochondrial Membrane Potential and ROS Accumulation Assay. A lipophilic cationic dye, 5,5′,6,6′-tetrachloro-1,1′,3,3′-tetraethylbenzimidazolcarbocyanine (JC-1, Beyotime, China), was used to monitor the level of MMP in the cells. At normal state, the MMP is high and JC-1 appears as aggregates, which is indicated by red fluorescence. However, when apoptosis occurs, the MMP reduced and JC-1 displayed as monomers, which is indicated by green fluorescence. We applied two methods which included flow cytometry and fluorescence microscopy to detect the MMP. For flow cytometry analysis, A549 cells were plated in six-well plates (3×10^5 cells/well) and grown for 24 h and treated with compound **25a** at the indicated concentrations for 24 h. Then the cells were harvested by centrifugation and incubated with JC-1 solution for 30 min. After brief washing, the proportion of green and red fluorescence intensity was immediately detected and analyzed by flow cytometry. For the fluorescence microscopy detection, A549 cells were plated in a confocal culture dish at 5×10^4 cells/dish and grown for 24 h and treated with compound **25a** at the indicated concentrations for another 24 h. Then the cells were stained with 2 μM JC-1 at 37 °C for 30 min, washed with PBS, and then the cell nuclei were stained with Hoechst 33342 (Sigma, USA) for 10 min in the dark. The cell images were immediately detected by a Zeiss LSM 570 laser scanning confocal microscope (Carl Zeiss, Germany). The intracellular ROS accumulation assay was determined by fluorescence microscopy using the reactive oxygen species assay kit (ROS assay kit, Beyotime). A549 cells were cultured in six-well plates (3×10^5 cells/well) for 24 h. After adding compound **25a** for 12 h, the culture supernatants were removed, and the cells were then incubated with 10 mM DCFH-DA in fresh medium at 37 °C for 30 min. After incubation, the culture medium was removed, and the cells were washed with PBS buffer three times. The production of ROS could be measured by changes in the fluorescence intensity due to the intracellular accumulation of dichlorofluorescein (DCF) caused by the oxidation of DCFH. The intracellular ROS level, as indicated by the DCF fluorescence, was determined by measuring the fluorescence intensity on a multifunctional monochromator-based microplate reader with the excitation and emission wavelengths set at 488 and 525 nm, respectively. To observe the intracellular ROS level visually, we used the Arrayscan VTI high content analysis system to acquire cell images after the cell nuclei were stained with Hoechst 33342 (Sigma) for 10 min in dark conditions.

Anti-Cell-Migration Study. A549 or PC9 cells were plated in a six-well culture dish at 5×10^4 cells/dish and grown for 24 h, and the nonmigrated cells were scraped off the upper surface of the membrane with a 10 μL pipet. The medium was then replaced with serum-free DMEM medium and treated with compound **23a**, **25a**, and **25d** at the indicated concentrations for another 24 h. After the samples were washed with phosphate buffer solution (PBS), the cell images were immediatelt detected by a Zeiss LSM 570 laser scanning confocal microscope (Carl Zeiss, Germany).

Statistical Analysis. All data are presented as the mean ± SD (standard deviations). Statistical significance between the control and test groups was evaluated by Student's test. The differences were considered statistically significant when $P < 0.05$.

Evaluation of in Vivo Antitumor Activity. Animals and Implantation of Cancer Cells. Male BALB/c nude mice (5 weeks old, 18−20 g) were purchased and housed at the Laboratory Animal Service Center of Sun Yat-Sen University (Guangzhou, China) in pathogen-free condition, maintained at constant room temperature, and fed a standard rodent chow and water. 1×10^7 cells/mL A549 cells grown in logarithmic phase were harvested and resuspended in FBS-free DMEM medium. Then, 0.1 mL of the cell suspension was subcutaneously injected into the right flank of each mouse. After implantation, the tumor mass was measured with an electronic caliper twice a week, and the tumor volume was calculated according to the following formula: tumor volume (mm^3) = 0.5 × length × $width^2$.

Acute Toxicity Experiment. Male Kunming mice (5 weeks old, 18−24 g) were purchased and housed at the Laboratory Animal Service Center of Sun Yat-Sen University (Guangzhou, China) in pathogen-free condition, maintained at constant room temperature, and fed a standard rodent chow and water. The mice were randomly divided into experimental group and control group. The experimental group was divided into 15 groups, each with 4 males, according to A−D sequence number. Then, the mice were caudal vein injected with CA-4P at a dose of 30/175/300 mg/kg, with compounds **23a**·HCl, **25a**·HCl, **25d**·HCl, and EP128495·HCl at a dose of 3/17.5/300 mg/kg.The control group was caudal vein injected with NaCl solution.

Drug Treatments and Evaluation of in Vivo Antitumor Activity. When the tumor volume reached about 100 mm^3, the xenograft tumor-bearing nude mice were randomly allocated to six

DOI: 10.1021/acs.jmedchem.8b00128
J. Med. Chem. XXXX, XXX, XXX−XXX

groups (vehicle-treated, CA-4P-treated, EP128495-treated, **23a**-treated, **25a**-treated, and **25d**-treated groups), with 5 mice per group. Then, the mice were intraperitoneally injected with CA-4P at a dose of 30 mg/kg, compounds **23a**, **25a**, **25d**, and EP128495 at a dose of 2.5 mg/kg every 2 days for the entire observation period, and the control group was treated with an equivalent volume of vehicle. Tumor volume and body weights were recorded every 2 days after drug treatment. At the end of the observation period, the animals were euthanized by cervical dislocation and the tumor bulks were peeled off, conforming to the Guide for the Care and Use of Laboratory Animals as published by the U.S. National Institutes of Health (NIH Publication No. 85-23, revised 1996) and approved by the Institutional Ethics Review Board of Sun Yat-Sen University.

■ ASSOCIATED CONTENT

Supporting Information

The Supporting Information is available free of charge on the ACS Publications website at DOI: 10.1021/acs.jmedchem.8b00128.

Molecular formula strings and some data (CSV)

■ AUTHOR INFORMATION

Corresponding Authors

*L.H.: phone, +086-20-3994-3050; fax, +086-20-3994-3050; e-mail, Huangl72@mail.sysu.edu.cn.

*X.L.: phone, +086-20-3994-3050; fax, +086-20-3994-3050; e-mail, lixsh@mail.sysu.edu.cn.

ORCID

Xingshu Li: 0000-0002-7433-739X

Notes

The authors declare no competing financial interest.

■ ACKNOWLEDGMENTS

We thank the National Natural Science Foundation of China (Grants 21772241 and 21302235), Guangdong Natural Science Foundation (Grant 2014A030313124), Guangdong High-Level Personnel of Special Support Program, Young Top-Notch Talent Project (Grant 2015TQ01R244), Guangzhou Pearl River New Star Fund Science and Technology Planning Project (Grant 201610010111), and The Fundamental Research Funds for the Central Universities (Grant 15ykpy04) for financial support of this study.

■ ABBREVIATIONS USED

SAR, structure−activity relationship; TLC, thin-layer chromatography; MOM, methyl−oxygen−methyl; IPA, isopropanol; DIPEA, diisopropylethylamine; DMSO, dimethyl sulfoxide; Pgp, P-glycoprotein; MDR, multidrug resistant; ROS, reactive oxygen species; MMP, mitochondrial membrane potential; NSCLC, non-small-cell lung carcinoma; CA-4P, combretastatin A-4 phosphorus; FBS, fetal bovine serum; DAPI, 4′,6-diamidino-2-phenylindole; PBS, phosphate buffer solution; SDS−PAGE, sodium dodecyl sulfate−polyacrylamide gel electrophoresis; DCFH-DA, 2′,7′-dichlorodihydrofluorescein diacetate; DCF, dichlorofluorescein; FITC, fluorescein isothiocyanate; PI, propidium iodide; DOX, doxorubicin; CDDP, cis-platinum; MTT, 3-(4,5-dimethylthiazol-2-yl)-2,5-diphenyltetrazolium bromide; JC-1, 5,50,6,60-tetrachloro-1,10,3,30-tetraethylbenzimidazolcarbocyanine; EGTA, ethylene glycol tetraacetic acid; GTP, guanosine triphosphate

■ REFERENCES

(1) Horio, T.; Murata, T. The role of dynamic instability in microtubule organization. *Front. Plant Sci.* **2014**, *5*, 511.

(2) Pellegrini, F.; Budman, D. R. Review: tubulin function, action of antitubulin drugs, and new drug development. *Cancer Invest.* **2005**, *23*, 264−273.

(3) Prota, A. E.; Bargsten, K.; Zurwerra, D.; Field, J. J.; Díaz, J. F.; Altmann, K.-H.; Steinmetz, M. O. Molecular mechanism of action of microtubule-stabilizing anticancer agents. *Science* **2013**, *339*, 587−590.

(4) Stanton, R. A.; Gernert, K. M.; Nettles, J. H.; Aneja, R. Drugs that target dynamic microtubules: a new molecular perspective. *Med. Res. Rev.* **2011**, *31*, 443−481.

(5) Dumontet, C.; Jordan, M. A. Microtubule-binding agents: a dynamic field of cancer therapeutics. *Nat. Rev. Drug Discovery* **2010**, *9*, 790−803.

(6) Jordan, M. A.; Wilson, L. Microtubules as a target for anticancer drugs. *Nat. Rev. Cancer* **2004**, *4*, 253−265.

(7) Kasibhatla, S.; Baichwal, V.; Cai, S. X.; Roth, B.; Skvortsova, I.; Skvortsov, S.; Lukas, P.; English, N. M.; Sirisoma, N.; Drewe, J.; Pervin, A.; Tseng, B.; Carlson, R. O.; Pleiman, C. M. MPC-6827: a small-molecule inhibitor of microtubule formation that is not a substrate for multidrug resistance pumps. *Cancer Res.* **2007**, *67*, 5865−5871.

(8) Chamberlain, M. C.; Grimm, S.; Phuphanich, S.; Recht, L.; Zhu, J. Z.; Kim, L.; Rosenfeld, S.; Fadul, C. E. A phase 2 trial of verubulin for recurrent glioblastoma: a prospective study by the brain tumor investigational consortium (BTIC). *J. Neuro-Oncol.* **2014**, *118*, 335−343.

(9) Prabhu, K. S.; Lei, X. G. *Adv. Nutr.* **2016**, *7*, 415−7.

(10) Kryukov, G. V.; Castellano, S.; Novoselov, S. V.; Lobanov, A. V.; Zehtab, O.; Guigó, R.; Gladyshev, V. N. Characterization of mammalian selenoproteomes. *Science* **2003**, *300*, 1439−1443.

(11) Allmang, C.; Wurth, L.; Krol, A. The selenium to selenoprotein pathway in eukaryotes: more molecular partners than anticipated. *Biochim. Biophys. Acta, Gen. Subj.* **2009**, *1790*, 1415−14123.

(12) Vinceti, M.; Crespi, C. M.; Malagoli, C.; Del Giovane, C.; Krogh, V. Friend. The current epidemiologic evidence on selenium and human cancer risk. *J. Environ. Sci. Health C Environ. Carcinog Ecotoxicol Rev.* **2013**, *31*, 305−341.

(13) Sharma, A. K.; Amin, S. Post select: selenium on trial. *Future Med. Chem.* **2013**, *5*, 163−174.

(14) Chung, C. Y.; Madhunapantula, S. V.; Desai, D.; Amin, S.; Robertson, G. P. Melanoma prevention using topical PBISe. *Cancer Prev. Res.* **2011**, *4*, 935−948.

(15) Lin, T.; Ding, Z.; Li, N.; Xu, J.; Luo, G.; Liu, J.; Shen, J. Seleno-cyclodextrin sensitises human breast cancer cells to TRAIL-induced apoptosis through DR5 induction and NF-kappaB suppression. *Eur. J. Cancer* **2011**, *47*, 1890−1907.

(16) Nguyen, N.; Sharma, A.; Nguyen, N.; Sharma, A. K.; Desai, D.; Huh, S. J.; Amin, S.; Meyers, C.; Robertson, G. P. Melanoma chemoprevention in skin reconstructs and mouse xenografts using isoselenocyanate-4. *Cancer Prev. Res.* **2011**, *4*, 248−258.

(17) Yang, Y.; Huang, F.; Ren, Y.; Xing, L.; Wu, Y.; Li, Z.; Pan, H.; Xu, C. The anticancer effects of sodium selenite and selenomethionine on human colorectal carcinoma cell lines in nude mice. *Oncol. Res.* **2009**, *18*, 1−8.

(18) Zeng, H.; Cheng, W. H.; Johnson, L. K. Methylselenol, a selenium metabolite, modulates p53 pathway and inhibits the growth of colon cancer xenografts in Balb/c mice. *J. Nutr. Biochem.* **2013**, *24*, 776−780.

(19) dos Santos, E. d. A.; Hamel, E.; Bai, R.; Burnett, J. C.; Tozatti, C. S. S.; Bogo, D.; Perdomo, R. T.; Antunes, A. M. M.; Marques, M. M.; Matos, M. F. C.; de Lima, D. P. Synthesis and evaluation of diaryl sulfides and diaryl selenide compounds for antitubulin and cytotoxic activity. *Bioorg. Med. Chem. Lett.* **2013**, *23*, 4669−4673.

(20) Guan, Q.; Yang, F.; Guo, D.; Xu, J.; Jiang, M.; Liu, C.; Bao, K.; Wu, Y.; Zhang, W. Synthesis and biological evaluation of novel 3,4-diaryl-1,2,5-selenadiazol analogues of combretastatin A-4. *Eur. J. Med. Chem.* **2014**, *87*, 1−9.

DOI: 10.1021/acs.jmedchem.8b00128
J. Med. Chem. XXXX, XXX, XXX−XXX

(21) Plano, D.; Karelia, D. N.; Pandey, M. K.; Spallholz, J. E.; Amin, S.; Sharma, A. K. Design, synthesis, and biological evaluation of novel selenium (Se-NSAID) molecules as anticancer agents. *J. Med. Chem.* **2016**, *59*, 1946−1959.
(22) Brown, K. M.; Arthur, J. R. Selenium, selenoproteins and human. *Public Health Nutr.* **2001**, *4*, 593−599.
(23) Terry, P. D.; Qin, B.; Camacho, F.; Moorman, P. G.; Alberg, A. J.; Barnholtz-Sloan, J. S.; Bondy, M.; Cote, M.L.; Funkhouser, E.; Guertin, K. A.; Peters, E. S.; Schwartz, A. G.; Schildkraut, J. M.; Bandera, E. V. Supplemental selenium may decrease ovarian cancer risk in African-American women. *J. Nutr.* **2017**, *147*, 621−627.
(24) Rayman, M. P. Selenium in cancer prevention: a review of the evidence and mechanism of action. *Proc. Nutr. Soc.* **2005**, *64*, 527−542.
(25) Boussada, M.; Ali, R. B.; Said, A. B.; Bokri, K.; Akacha, A. B.; Dziri, C.; El May, M. V. Selenium and a newly synthesized thiocyanoacetamide reduce doxorubicin gonadotoxicity in male rat. *Biomed. Pharmacother.* **2017**, *89*, 1005−1017.
(26) Li, H.; Li, F.; Yang, F.; Fang, Y.; Xin, Z.; Zhao, Li.; Hu, Q. Size effect of Se-enriched green tea particles on in vitro antioxidant and antitumor activities. *J. Agric. Food Chem.* **2008**, *56*, 4529−4533.
(27) Aylett, C. H.; Lowe, J.; Amos, L. A. New insights into the mechanisms of cytomotive actin and tubulin filaments. *Int. Rev. Cell Mol. Biol.* **2011**, *292*, 1−71.
(28) Liu, C.; Fu, Y.; Li, C.; Chen, T.; Li, X. Phycocyanin-functionalized selenium nanoparticles reverse palmitic acid-induced pancreatic β cell apoptosis by enhancing cellular uptake and blocking reactive oxygen species (ROS)-mediated mitochondria dysfunction. *J. Agric. Food Chem.* **2017**, *65*, 4405−4413.
(29) Li, W. J.; Nie, S. P.; Yao, Y. F.; Liu, X. Z.; Shao, D. Y.; Gong, D. M.; Cui, S. W.; Phillips, G. O.; He, M.; Xie, M. Y. Ganoderma atrum polysaccharide ameliorates hyperglycemia-induced endothelial cell death via a mitochondria-ROS pathway. *J. Agric. Food Chem.* **2015**, *63*, 8182−8191.
(30) Juan, M. E.; Wenzel, U.; Daniel, H.; Planas, J. M. Resveratrol induces apoptosis through ROS-dependent mitochondria pathway in HT-29 human colorectal carcinoma cells. *J. Agric. Food Chem.* **2008**, *56*, 4813−4818.

DOI: 10.1021/acs.jmedchem.8b00128
J. Med. Chem. XXXX, XXX, XXX−XXX